Materials Today Sustainability 33 (2026) 101282

Contents lists available at ScienceDirect

Materials Today Sustainability

journal homepage: www.journals.elsevier.com/materials-today-sustainability

Hydrogen embrittlement in storage tank materials and welded joints

Ammar Elsheikh [a,b,*], Ali Ali [c], Fadl A. Essa [d], Mohamed A.E. Omer [e,a], Mohamed G. Abou-Ali [f,g], Ninshu Ma [b,**]

[a] Production Engineering Department, Faculty of Engineering, Tanta University, Tanta, 41427, Egypt
[b] Joining and Welding Research Institute, University of Osaka, 51-4 Mihogaoka, Ibaraki, Osaka, 463-0057, Japan
[c] Advanced Technical College, University of Warith Al-Anbiyaa, Karbala, Iraq
[d] Mechanical Engineering Department, Faculty of Engineering, Kafrelsheikh University, Kafrelsheikh, 33516, Egypt
[e] Department of Mechanical and Aerospace Engineering, College of Engineering, United Arab Emirates University, Al Ain, 15551, United Arab Emirates
[f] Production Engineering Department, Faculty of Engineering, Alexandria University, Egypt
[g] Faculty of Engineering, Pharos University in Alexandria, Alexandria 21648, Egypt

ARTICLE INFO

Keywords:
Hydrogen embrittlement
Welded joints
Hydrogen storage tanks
Material degradation
Clean energy

ABSTRACT

Hydrogen embrittlement (HE) poses a significant threat to the structural integrity and long-term reliability of its storage tanks, particularly in welded joints, where microstructural heterogeneities increase susceptibility. This review presents a comprehensive analysis of HE phenomena, emphasizing its critical role in material degradation. The paper begins by outlining the fundamentals of HE, describing how atomic hydrogen infiltrates metallic lattices, leading to loss of ductility and premature failure. Various HE mechanisms, including hydrogen-enhanced decohesion (HEDE), hydrogen-enhanced localized plasticity (HELP), and hydrogen-induced cracking (HIC), are discussed and classified based on their underlying physical principles. The susceptibility of commonly used storage tank materials, such as high-strength steels and aluminum alloys, is evaluated, with a focus on microstructural and compositional factors. Special attention is given to the welded regions, where residual stresses, grain boundary structures, and weld metal (WM) composition play a pivotal role in accelerating HE. The review also highlights key factors influencing HE in welded joints, including hydrogen diffusion pathways, welding processes, and post-weld treatments. Experimental methodologies, such as slow strain rate testing and thermal desorption analysis, are discussed alongside simulation approaches that model hydrogen diffusion and crack propagation. Finally, the paper outlines current mitigation strategies, including material selection, heat treatment, hydrogen barriers, and cathodic protection, offering insights into practical solutions for reducing HE risks in hydrogen storage systems. This review aims to guide future research and inform engineering practices for safer hydrogen infrastructure.

Nomenclature

Symbols	
a	Crack length
b	Crack depth
C	Hydrogen concentration
D	Diffusion coefficient
D_0	Pre-exponential factor
E_a	Activation energy
E_d	Trap energy (desorption)
E_t	Trap energy (capture)
H_2S	Hydrogen sulfide
K	Trap equilibrium constant
k	Trapping rate
p	Trap release rate
T	Temperature
Ti	Titanium
t	Thickness
V	Vanadium
V_m	Partial molar volume of hydrogen
W	Specimen width
Zr	Zirconium
σ_h	Hydrostatic stress

(continued on next column)

(continued)

(continued on next page)

* Corresponding author. Production Engineering Department, Faculty of Engineering, Tanta University, Tanta, 41427, Egypt.
** Corresponding author.
E-mail addresses: ammar_elsheikh@f-eng.tanta.edu.eg (A. Elsheikh), ma.ninshu.jwri@osaka-u.ac.jp (N. Ma).

https://doi.org/10.1016/j.mtsust.2025.101282
Received 22 May 2025; Received in revised form 14 October 2025; Accepted 17 December 2025
Available online 20 December 2025

(*continued*)

$\Delta\delta$	Elongation loss
$\Delta\sigma$	Tensile strength loss
$\nabla\sigma_h$	Stress gradient
θ	Lattice site occupancy
ϑ	Trap occupancy
Abbreviations	
AF	Acicular Ferrite
BM	Base metal
CGHAZ	Coarse-grained heat-affected zone
CLR	Crack length ratio
CSR	Crack sensitivity ratio
CTR	Crack thickness ratio
DP	Dual-phase
FEA	Finite element method
FGHAZ	Fine-grained heat-affected zone
FSW	Friction stir welding
GBE	Grain boundary engineering
GBs	Grain boundaries
GMAW	Gas metal arc welding
GTAW	Gas tungsten arc welding
HAC	Hydrogen-Assisted Creep
HAF	Hydrogen-assisted fatigue
HAGBs	High-angle grain boundaries
HAs	Hydrogen atoms
HAZ	Heat-affected zones
HE	Hydrogen embrittlement
HEA	High-entropy alloy
HEDE	Hydrogen-enhanced decohesion
HELP	Hydrogen-enhanced localized plasticity
HF	Hydride formation
HIB	Hydrogen-induced blistering
HIC	Hydrogen-induced cracking
HIF	Hydrogen-induced fracture
HIPT	Hydrogen-induced phase transformations
HISC	Hydrogen-induced stress cracking
LBW	Laser beam welding
L-PBF	Laser Powder Bed Fusion
MIG	Metal inert gas
MLG	Multi-layered graphene
NZ	Nugget zone
SSRT	Slow strain rate test
TDS	Thermal desorption spectroscopy
TIG	Tungsten inert gas
TWIP	Twinning-induced plasticity
WM	Weld metal
XRD	X-ray diffraction

1. Introduction

The development of green technologies is a crucial goal for humanity [1]. As the world confronts the urgent challenge of environmental degradation, creating renewable and eco-friendly energy resources has become a central priority [2]. A sustainable future hinge on reducing the harmful impacts of conventional energy sources and transitioning toward cleaner alternatives [3]. To achieve this transition toward cleaner energy, diverse energy conversion and storage technologies are being developed to form the foundation of sustainable power systems. These include lithium-ion batteries [4,5], supercapacitors [6], fuel cells [7], and emerging solid-state and bio-inspired systems [8], each offering distinct advantages in terms of energy density, efficiency, and scalability. Moreover, integrated systems such as self-powered electrochemical energy storage [9] and microfluidic platforms [10]for electrochemical conversion are gaining attention for their potential in portable and on-demand applications.

Additionally, hydrogen has emerged as a promising solution, capturing considerable interest from researchers and policymakers [11]. Hydrogen, being one of the most abundant elements in nature, holds immense potential as a clean and efficient energy source [12]. When it undergoes oxidation, it releases three times more energy per unit mass compared to the combustion of traditional hydrocarbons, making it a far more efficient option [13]. Importantly, the only byproduct of hydrogen combustion is water, which makes it an environmentally safe alternative to fossil fuels [14]. As global focus shifts to renewable energy, hydrogen stands out for its versatility and clean energy potential [15]. Produced through electrolysis from renewable sources like solar, wind, and hydropower, hydrogen can be created without carbon emissions [16]. It has the potential to replace fossil fuels and reduce greenhouse gases, with water vapor being the only byproduct when used in fuel cells or for energy. Hydrogen is key in diverse applications, from powering vehicles to industrial processes, and is especially valuable in sectors like heavy industry, aviation, and shipping, where electrification is difficult. With increasing demand and advancements in hydrogen production and storage, it is set to become a dominant energy source, offering a cleaner, greener solution for a carbon-neutral future. However, despite its potential, one of the main challenges with hydrogen is its storage [17]. At standard temperature and pressure, hydrogen has a low energy density, meaning it needs to be stored in a compact and efficient way to be used effectively in practical applications [18]. This highlights the critical importance of hydrogen storage. There are various methods of storing hydrogen, each with its own advantages and challenges. Compressed hydrogen, stored in high-pressure tanks, is currently the most common method for both transportation and stationary applications [19]. Another promising approach is liquefied hydrogen, which involves cooling the gas to extremely low temperatures [20]. This method is more energy-dense, but it requires sophisticated infrastructure and energy-intensive cooling processes. Solid-state hydrogen storage, through materials like metal hydrides, offers another route but is still in the developmental phase [21].

Effective hydrogen storage systems are essential not only for ensuring the feasibility of hydrogen-based technologies but also for enabling a hydrogen economy [22]. The ability to store large quantities of hydrogen safely and efficiently can facilitate its use in fluctuating energy markets, where it can act as a medium for storing excess renewable energy produced during periods of high generation, such as windy or sunny days. This stored hydrogen can then be converted back into electricity or used in various other applications when demand is high or renewable generation is low. For this reason, advancing hydrogen storage technologies is a critical step toward unlocking the full potential of hydrogen as a clean energy carrier and ensuring a sustainable and resilient energy future [23].

HE is a phenomenon where materials, particularly metals, become brittle and prone to cracking or failure when exposed to hydrogen [24]. This occurs when hydrogen atoms (HAs) diffuse into the metal's structure, causing changes in its mechanical properties. Over time, the metal becomes weaker, more prone to fracture, and may fail under stress, even at lower loads than it would under normal conditions. The process of hydrogen absorption into a material typically weakens the atomic bonds, resulting in a loss of ductility and an increased risk of fracture. HE is a critical consideration for industries dealing with hydrogen, as it can compromise the integrity and safety of equipment designed to store, transport, or utilize hydrogen gas [25].

In the context of hydrogen storage tanks, the risk of HE is particularly significant [26]. Storage tanks are designed to hold hydrogen under high pressure, which intensifies the potential for HAs to infiltrate the materials used in the tank's construction. Metals like steel and aluminum, commonly used in tank fabrication, are especially vulnerable to HE when exposed to hydrogen gas, particularly under high pressure and at elevated temperatures. As hydrogen diffuses into the material, it can form microscopic cracks or fissures that can propagate, leading to catastrophic failure if not properly managed. Therefore, understanding and mitigating HE is critical in ensuring the safety and longevity of hydrogen storage systems [27]. HE impacts the selection and design of storage tank materials. Engineers must consider hydrogen's effects when choosing materials, often opting for high-strength steels or composites to resist cracking. However, these materials must be carefully evaluated for their susceptibility to embrittlement. To improve resistance, strategies like surface coatings, alloying, and using carbon fiber composites are explored. These measures are crucial for ensuring hydrogen storage

systems are safe, reliable, and durable.

Despite the growing adoption of hydrogen as a clean energy carrier, HE in storage tanks; particularly in welded joints; remains a critical challenge for infrastructure safety and durability. Welded regions are inherently more vulnerable than base materials due to localized microstructural changes, residual stresses, and hydrogen diffusion pathways introduced during welding. While numerous studies have addressed HE in bulk materials, comparatively fewer have examined welded joints, and existing research often treats HE mechanisms in isolation without fully considering the combined influence of welding processes, post-weld treatments, and environmental conditions. Okonkwo et al. [28] provided a concise overview of HE mechanisms in hydrogen storage tanks, emphasizing degradation processes and some mitigation strategies. However, their review did not address hydrogen embrittlement and its implications for welded joints. Sun and Cheng's [29] review primarily addressed hydrogen-induced degradation in high-strength steel pipeline welds, with particular emphasis on diffusion–trapping mechanisms, microstructural heterogeneity, and computational models for assessing pipeline integrity. Nevertheless, their analysis was confined to pipeline welds and did not extend to hydrogen storage tanks. Extending the pipeline perspective, Jia et al. [30] provided a broader overview of hydrogen embrittlement in hydrogen-blended natural gas systems, addressing infrastructure-wide challenges but without a dedicated focus on hydrogen storage tanks. Yu et al. [31] provided a comprehensive review focused on HE in both hydrogen storage tanks and gas transportation systems, emphasizing fundamental mechanisms, atomistic modeling, and emerging materials; however, the specific influence of HE on welded joints was not examined in detail.

Building on these gaps, this review consolidates and critically analyzes current knowledge on HE, focusing on welded joints where mechanisms such as HEDE, HELP, and HIC act concurrently to degrade ductility and fracture resistance. Experimental investigations and modeling approaches demonstrate that material susceptibility varies with alloy composition and welding procedure, while mitigation strategies such as post-weld heat treatment, protective coatings, and alloy optimization can reduce but not completely eliminate embrittlement risks. The findings highlight that no single solution is universally effective; instead, an integrated approach is required to enhance the long-term reliability of hydrogen storage systems.

2. Types of hydrogen tanks

HE is a critical consideration for industries dealing with hydrogen, as it can compromise the integrity and safety of equipment designed to store, transport, or utilize hydrogen gas [25]. Among the most vulnerable components are the hydrogen storage tanks (HSTs), where the risk of HE is particularly significant [26]. These tanks are engineered in various configurations, ranging from all-metal to fully composite designs, each tailored to balance pressure capacity, weight, manufacturing complexity, and application suitability. Table 1 provides an overview of the primary classifications of HSTs, their design characteristics, and their typical application environments. HE and corrosion are major concerns for metallic hydrogen storage tanks, especially Types I, II, and III. HE occurs when HAs diffuse into metals like steel and aluminum, weakening their structure and making them brittle, particularly under high pressure. Over time, this can lead to cracks and structural failure. Corrosion, caused by chemical reactions with elements like moisture or salt, gradually degrades metal surfaces—even in resistant materials like stainless steel. In hydrogen storage, corrosion can cause leaks or wall weakening, compromising tank integrity. Both issues require ongoing monitoring, maintenance, and protective measures to ensure safe operation.

Welding joints are commonly used in the construction of hydrogen storage tanks, especially to join the various components such as the tank's shell, nozzles, and fittings. However, the use of welding in these tanks requires careful consideration due to the unique challenges posed by hydrogen, particularly HE and the risk of corrosion. Welding creates a fusion between metal parts, and in the case of hydrogen storage tanks, these joints are critical for maintaining the integrity of the tank under high-pressure conditions. One of the primary concerns when welding hydrogen storage tanks is HE. This occurs when HAs infiltrate the metal

Table 1
Overview of HSTs design, pressure ratings, and performance characteristics [32–34].

Type	Construction	Pressure (bar)	Advantages	Limitations
Type I 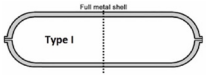 (All-metal)	Made entirely of metal (e.g., steel or aluminum)	▪ Al: 175 ▪ Steel: 200	▪ Simple and robust design ▪ Easy to manufacture	▪ Heaviest type ▪ Lower storage efficiency (weight-to-gas ratio) ▪ Not ideal for mobile applications (e.g. vehicles)
Type II 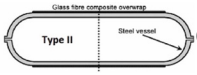 (Hoop-wrapped)	Metal liner + hoop-wrapped fiberglass or carbon fiber	▪ Al/glass: 263 ▪ Steel/carbon fibre: 299	▪ Lighter than Type I due to partial composite wrapping ▪ Better weight-to-storage efficiency ▪ Cheaper than fully composite tanks	▪ Still relatively heavy ▪ Limited pressure rating compared to fully wrapped types
Type III 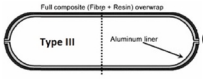 (Fully-wrapped + metal)	Metal liner + fully-wrapped composite (e.g., carbon fiber)	Al/glass: 305 Al/aramid: 438 Al/carbon: 700	- Much lighter than Types I & II - Higher pressure tolerance	▪ More expensive than Type I and II
Type IV 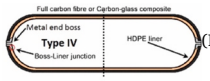 (Fully wrapped + polymer)	Polymer liner + fully-wrapped composite (typically carbon fiber)		▪ Very lightweight ▪ High corrosion resistance ▪ Excellent for mobile applications (e.g. vehicles)	▪ Requires complex manufacturing
Type V 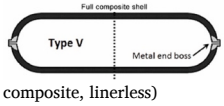 (All-composite, linerless)	Made entirely of composite material	1000	▪ Ultra-lightweight ▪ Maximum storage efficiency ▪ No corrosion issues ▪ Excellent for aerospace applications	▪ Very high cost ▪ Limited commercial availability ▪ Structural challenges with no liner

during the welding process, causing the material to become brittle and prone to cracking. Metals like steel and aluminum, which are commonly used in hydrogen tanks, are particularly vulnerable to this phenomenon, especially in high-stress or high-pressure environments. As a result, welding procedures must be carefully controlled to avoid introducing hydrogen into the material. Special welding electrodes, preheating of the material, and moisture control during welding are necessary to mitigate the risk of embrittlement and ensure the strength and durability of the welds.

Additionally, the choice of material is crucial when welding hydrogen storage tanks. Materials used for the welding process must be resistant to HE and corrosion, which are common issues in hydrogen environments. Stainless steel and aluminum alloys are often preferred for their ability to resist these issues. For tanks made of composite materials, such as Type II and Type III tanks, welding is typically used only for the metal liner, while the composite overwrap is bonded using other methods like adhesive bonding or filament winding.

The welding process itself also needs to be carefully managed. Techniques such as Tungsten Inert Gas (TIG) welding or Metal Inert Gas (MIG) welding are typically used in the construction of hydrogen storage tanks because they provide strong, clean joints that minimize defects. Any flaws in the weld could lead to leakage or failure of the tank under pressure. To ensure the integrity of the welded joints, non-destructive testing methods such as ultrasonic testing, X-ray inspection, and hydrogen leak detection are often employed to detect any potential weaknesses that could compromise the safety of the tank.

Another concern with welding is the creation of heat-affected zones (HAZ) around the weld. These areas, which experience a temperature change during the welding process, can alter the metal's properties, making it more susceptible to embrittlement or corrosion. In hydrogen storage tanks, these zones must be carefully controlled to ensure that they do not weaken the structure or lead to failure. In some cases, post-weld heat treatments or surface coatings are used to restore the material's strength and prevent further degradation.

Hydrogen permeation refers to the process by which HAs or molecules pass through a material, typically a membrane or a barrier. This phenomenon occurs due to the movement of HAs from an area of higher concentration to an area of lower concentration, driven by concentration gradients and, in some cases, pressure differences. Hydrogen permeation is an important factor in various industrial and scientific applications, such as hydrogen storage, fuel cells, and membrane technologies. Materials that are permeable to hydrogen can allow hydrogen to diffuse through them, which may be beneficial in certain applications (e.g., hydrogen purification or separation) or a potential problem (e.g., in pipelines or storage containers, where unwanted hydrogen leakage can occur).

There are several key steps involved in hydrogen permeation.

I. Adsorption: Hydrogen gas is absorbed onto the surface of the material.
II. Dissociation: Hydrogen molecules split into individual HAs on the surface of the material.
III. Diffusion: HAs move through the material's interior, often via mechanisms such as diffusion or through lattice sites in the material (in metals, this process is often diffusion-based).
IV. Desorption: The HAs are released from the opposite side of the material, recombining into hydrogen molecules.

Hydrogen permeation can be influenced by the properties of the material (such as its structure, temperature, and pressure), and materials that exhibit low hydrogen permeability are often sought for applications involving hydrogen storage or containment to prevent leaks and ensure safety.

3. Fundamentals of HE

3.1. HE and its impact on material degradation

HE reduces a metal's strength, ductility, and toughness due to hydrogen atom diffusion into its microstructure [24]. This can cause brittle phases, cracks, or voids, leading to issues like HIC or delayed fracture, depending on the material and conditions [35].

HE is a critical form of material degradation, as it weakens the structural integrity and safety of components exposed to hydrogen environments [36]. In industries such as energy, aerospace, and manufacturing, where high-strength materials are essential, hydrogen can cause premature failure of components under stress [37]. This is particularly concerning for applications like hydrogen storage and transport, where materials must remain strong and reliable under extreme conditions [26]. HE is especially dangerous because it can cause catastrophic failure without visible signs of damage, making early detection and prevention difficult [24]. As a result, understanding HE's mechanisms and its impact on material properties is essential for selecting, designing, and maintaining safer, more durable materials in hydrogen-related applications.

Fig. 1 illustrates the primary mechanisms and consequences of HE in metallic materials. HE initiates with hydrogen atom diffusion into the microstructure, leading to a reduction in strength, ductility, and toughness. It promotes defect formation such as cracks and voids, which compromise structural integrity and can result in sudden, undetectable failure. These effects are especially critical in high-strength alloys used in hydrogen storage and transport, emphasizing the need for careful material selection, stress control, and predictive maintenance to ensure long-term reliability.

3.2. Hydrogen charging methods

Hydrogen charging (HC) is commonly used to simulate real-world conditions to test material performance, particularly the susceptibility to hydrogen embrittlement, cracking, or other degradation mechanisms. The key parameters in HC include H-charge time, which affects the amount of hydrogen absorbed, the temperature, which influences the diffusion rate of H into the material, H-concentration, which affects the amount of hydrogen that can be absorbed, and pressure, which significantly influences absorption rates [38–40]. The common hydrogen charging methods include high-pressure HC, thermal charging, electrochemical charging, etc. [41–43]. In high-pressure HC, the material is exposed to hydrogen gas under high pressure, allowing hydrogen atoms to diffuse into the material. This method simulates the conditions that materials might experience in hydrogen-rich environments, such as in hydrogen storage systems or fuel cells. Thermal charging involves exposing the material to a hydrogen atmosphere at elevated temperatures. This technique is typically used to study hydrogen absorption at high temperatures; simulating conditions found in applications such as gas pipelines or high-temperature reactors. In electrochemical charging, hydrogen is introduced into a material by applying an electrical current to an electrolyte, which causes hydrogen ions to be reduced at the surface of the material. This method is commonly used in laboratory settings where precise control of hydrogen uptake is necessary. Zhao et al. [44] investigated the effects of HC methods, gaseous (G-) and electrochemical (E−) charging, on the hydrogen distribution and nanomechanical properties of CoCrFeMnNi high-entropy alloy (HEA) and compared it with 316 L austenitic stainless steel. Through thermal desorption spectroscopy (TDS) and nanoindentation experiments, they found that E-charging creates a steep hydrogen concentration gradient near the surface, leading to significant hardening (~63 % increase in hardness). In contrast, G-charging results in homogeneous hydrogen distribution throughout the material, causing negligible changes in mechanical properties despite higher total hydrogen content. The differences were attributed to the localized high hydrogen concentration

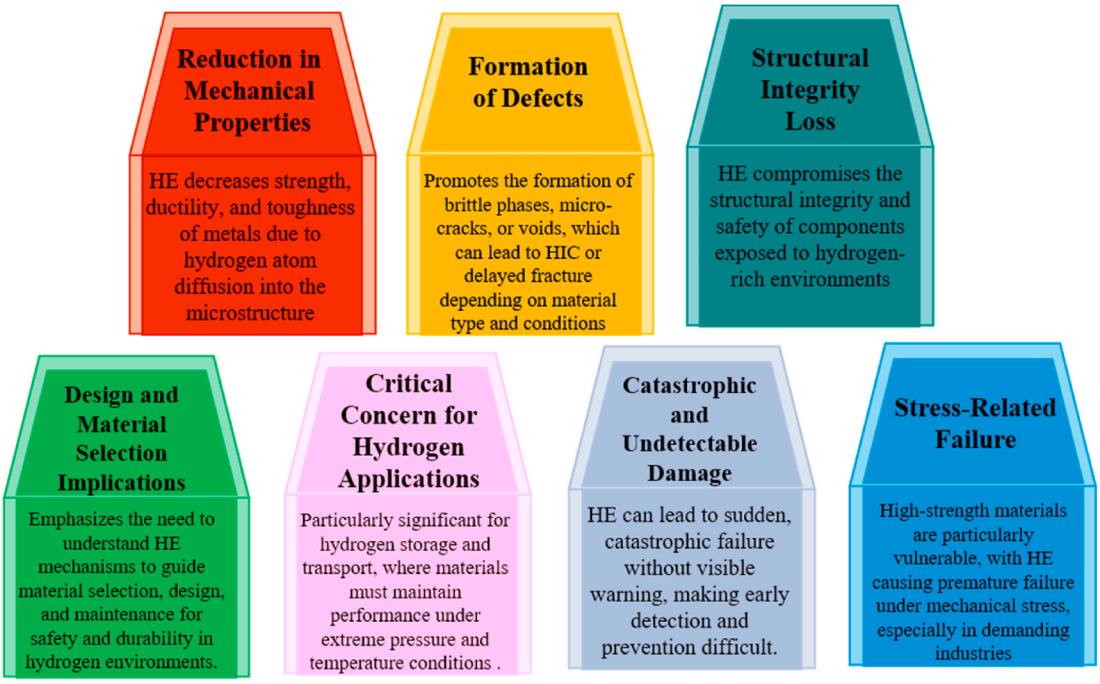

Fig. 1. Key aspects of material degradation due to HE.

near the surface in E-charged samples, which enhances solid solution strengthening and slip planarity, whereas the uniform distribution in G-charged samples does not reach the threshold for noticeable hardening. Fig. 2 shows a schematic representation of hydrogen atom distribution under G-charging and E-charging conditions, along with the nanoindentation hardness variations among uncharged, G-charged, and E-charged specimens. Rahimi et al. [45] conducted a comparative study on the HE of pipeline steels under slow and high strain rate tensile tests in both gaseous and electrolytic environments. They concluded that while both charging methods degrade ductility, E-charging generally results in greater embrittlement. Additionally, slower strain rates were found to enhance HE by allowing more time for hydrogen diffusion and interaction with dislocations. Microstructural features, including non-metallic inclusions and phase interfaces, were identified as critical factors influencing crack initiation and propagation. For welded samples, assessing the effects of hydrogen on different regions, such as the HAZ, base metal, and WM, is crucial. These regions often exhibit different susceptibilities to embrittlement due to variations in microstructure and residual stresses from the welding process. Feng et al. [46] investigate the HE behavior of the CoCrFeMnNi high-entropy alloy (HEA) in comparison with two conventional alloys, 304 stainless steel (304SS) and IN718. Through electrochemical hydrogen pre-charging, slow strain rate tensile tests, and fracture surface analysis, the authors demonstrate that the HEA exhibits superior resistance to hydrogen embrittlement under the tested conditions (1.79 mA cm^{-2} for 24 h and 48 h, and 179 mA cm^{-2} for 2 h). The hydrogen embrittlement index was lowest for the HEA, followed by 304SS and then IN718. Additionally, the ductility of the HEA was found to be dependent on hydrogen charging time: it increased after short charging periods due to hydrogen-enhanced twin formation, but decreased after longer charging due to the dominance of the hydrogen-enhanced decohesion (HEDE) mechanism. Ma et al. [47] explored the effects of electrochemical hydrogen charging on Q690 steel, focusing on current density and charging time's impact on HIB, cracking, and mechanical properties. Higher current densities lead to more and larger blisters, deeper cracks, and higher hydrogen concentrations, which increase active sites on the steel surface and initiate blister formation. At high densities (50 mA/cm^2), cracking shifts from mixed to intergranular modes, and mechanical properties degrade, causing a transition from ductile to brittle fracture. These findings highlight the increased sensitivity of

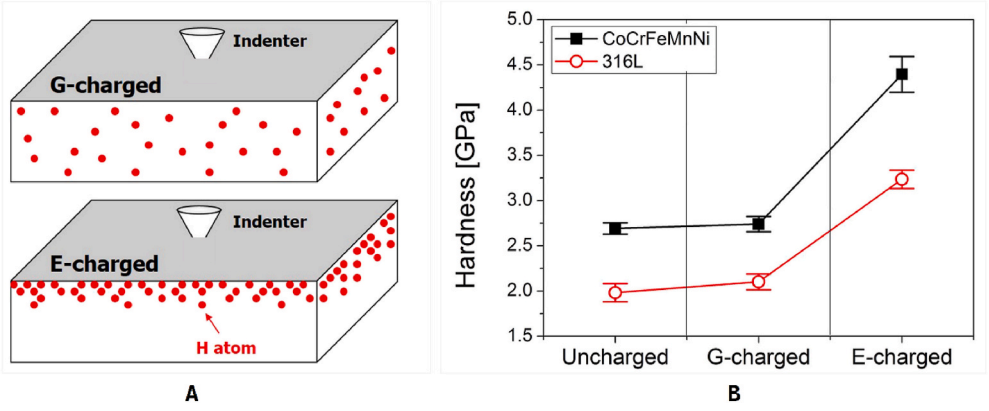

Fig. 2. (A) Schematic representation of hydrogen atom distribution under G-charging and E-charging conditions; (B) Nanoindentation hardness variations among uncharged, G-charged, and E-charged specimens [44].

Q690 steel to HE with higher charging conditions. The hydrogen concentration $C(x,t_c)$ at a depth x after a charging time t_c can be calculated using Eq. (1), where C_0 is the local hydrogen concentration at the surface of the H-charged specimen, D_H is the hydrogen diffusivity [44,48].

$$C(x,t_c) = C_0\left(1 - erf\left(\frac{x}{2\sqrt{D_H t_c}}\right)\right) \quad (1)$$

The surface concentration C_0 is given by Eq. (2):

$$C_0 = \frac{w \cdot C_M}{4}\sqrt{\frac{\pi}{D_H t_c}} \quad (2)$$

Where w is the sample thickness and C_M is the mean hydrogen concentration in the sample. The hydrogen trap density N_T (in cm^{-3}), which represents the number of hydrogen trapping sites per unit volume in a material, can be estimated using Eq. (3) [49]:

$$N_T = N_L\left(\frac{D_L}{D_{eff}}\right)e^{-\frac{E_b}{RT}} \quad (3)$$

where N_L is the density of interstitial lattice sites (cm^{-3}), D_L is the lattice diffusion coefficient (cm^2/s), D_{eff} is the effective diffusion coefficient (cm^2/s), E_b is the trap binding energy (eV), R is the universal gas constant, and T is the absolute temperature (K). This relation quantifies the number of hydrogen trapping sites based on the influence of diffusion and thermal activation.

● Ex-situ Vs. In-situ Testing Methodology

To assess how HE affects welded materials, researchers typically use two main HC techniques: ex-situ and in-situ, which are employed to introduce hydrogen into test specimens [50]. Ex-situ HC involves pre-charging the material with hydrogen before mechanical testing through one of the previously described methods. In contrast, in-situ HC introduces hydrogen during mechanical testing, enabling real-time observation of hydrogen-material interactions under stress. This method, however, presents a higher level of complexity in terms of setup, as it requires precise integration of hydrogen delivery systems with the mechanical testing apparatus as shown in Fig. 3 (A). Zafra et al. [52] conducted a study to compare hydrogen-assisted fatigue crack growth of welded 42CrMo4 steel under in-situ and ex-situ HC. In their work, they focused on both the base steel and the coarse-grain heat-affected zone (CGHAZ), which are known to exhibit different susceptibilities to HE due to their distinct microstructures. The study revealed that fatigue crack growth rates are significantly higher than an order of magnitude when samples are tested directly in a hydrogen-containing environment compared to pre-charged samples tested in air. This pronounced difference is attributed to the continuous supply of hydrogen at the crack tip during in-situ testing, which accelerates crack propagation. Notably, the CGHAZ consistently showed greater vulnerability to HE, regardless of the testing method. The differences between the two testing approaches are illustrated in Fig. 3 (B). The figure presents fatigue crack growth rate (da/dN) curves as a function of the stress intensity factor range (ΔK) for both the base steel and CGHAZ under various conditions: in air, after hydrogen pre-charging, and during in-situ exposure to hydrogen gas. As can be seen, for a given ΔK, the crack growth rates in the in-situ hydrogen environment are substantially higher than those observed in pre-charged specimens. This effect is especially pronounced at lower loading frequencies, where hydrogen has more time to diffuse to the crack tip, further accelerating crack propagation. Additionally, the figure highlights that the CGHAZ exhibits a steeper increase in crack growth rates compared to the base metal, underscoring its heightened susceptibility to hydrogen-assisted fatigue. Lee et al. [53] conducted a comprehensive investigation into the effect of EX-situ and In-situ on the mechanical behavior of a CoCrFeNi

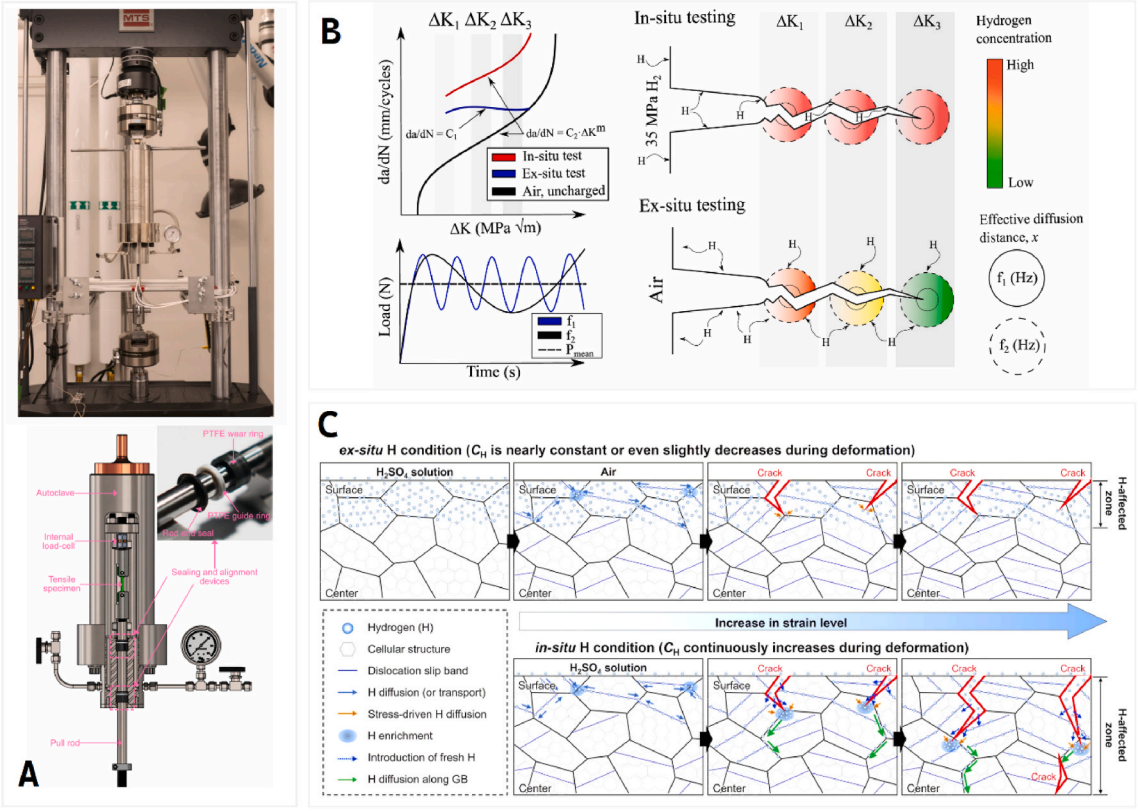

Fig. 3. (A) An example of a complex in-situ testing setup mounted on MTS servo-hydraulic load frame [51], (B) Effect of testing methodology (in-situ vs. ex-situ) on hydrogen accumulation and crack growth acceleration during fatigue, highlighting hydrogen loss in ex-situ tests and increased accumulation at lower loading frequencies (f_2) [52], and (C) Schematic illustration depicting the difference in hydrogen permeation under in-situ and ex-situ hydrogen charging conditions [53].

high-entropy alloy (HEA) fabricated by laser powder bed fusion (L-PBF). In the ex-situ condition, hydrogen was electrochemically pre-introduced into the specimen and then mechanically tested in air. This setup results in hydrogen becoming largely immobilized at relatively shallow depths, primarily in weak traps like dislocations and some grain boundaries. Thermal desorption spectroscopy (TDS) revealed that hydrogen uptake in this case was limited (~5.7 wt ppm), and microstructural damage was mostly confined to the near-surface region. By contrast, the in-situ condition, where hydrogen charging continues concurrently with tensile testing, produced significantly higher hydrogen uptake (~9.72 wt ppm), along with deeper and more aggressive crack penetration. Fig. 3 (C) represents a detailed schematic illustration of hydrogen permeation under both in-situ and ex-situ HC conditions. Hydrogen diffusion in the ex-situ condition is limited to slow lattice diffusion, which, based on Fick's law and reported diffusivity values ($\sim 3.7 \times 10^{-16}\ m^2/s$), leads to a shallow affected zone of just a few micrometers. In contrast, the depth of hydrogen permeation under in-situ HC,reached nearly 500 μm, corresponding to approximately half the sample's thickness. Christ et al. [54] studied the HE susceptibility of S690QL HSLA steel base material and gas metal arc welds using SSRT with in-situ HC. The effects of heat input on HE susceptibility were examined by welding with two different heat inputs. Results showed a significant loss of fracture elongation in hydrogen-charged specimens. Higher heat input led to WM with lower yield strength, increased ductility, and higher HE susceptibility due to a sharp hardness gradient in the CGHAZ. Gou [55] investigated the HIC behavior in the CGHAZ of X80 steel welds using in-situ HC tensile experiments, hydrogen permeation tests, and surface analysis techniques. The results showed that even small amounts of hydrogen can significantly reduce the material's elongation and area reduction. At a heat input of 29.2 kJ/cm, the steel showed minor HE sensitivity, with ductile fractures in the absence of hydrogen and brittle fractures when hydrogen was present. As heat input increased, the fracture mode transitioned from intergranular to a mixed intergranular-transgranular fracture, and eventually to transgranular fracture. The CGHAZ exhibited weak HE resistance, especially in the lath bainite structure, while GRB showed lower susceptibility to HE. Increased hydrogen concentration led to a rise in the Young's modulus of the base material but had less impact on the CGHAZ. The ultimate tensile strength (UTS) of CGHAZ decreased as hydrogen concentration increased.

3.3. Classification of HE mechanisms

HE poses a critical challenge to the structural integrity of welded storage tanks, often leading to catastrophic failures without visible warning signs. This phenomenon arises when atomic hydrogen infiltrates the material, interacting with the microstructure to induce a brittle fracture, reduced ductility, or delayed cracking. The mechanisms by which hydrogen degrades mechanical properties are complex and depend on material composition, welding-induced residual stresses, and environmental exposure. This section provides a foundation for understanding material behavior under hydrogen exposure and the subsequent protective strategies. Hydrogen-related damage mechanisms (refer to Fig. 4) can be broadly classified into the several types based on the interaction between hydrogen and the material's microstructure [56–59]. Table 2 provides an overview of various hydrogen-related damage mechanisms, the types of materials most susceptible to each, the environmental conditions under which these mechanisms typically occur, and effective mitigation strategies. Hydrogen embrittlement resistance can be assessed through the analysis of elongation (Δδ, %) and tensile strength (Δσ, %) losses at different stress levels, as described by Eq. (1) and Eq. (2) [95].

$$\Delta\delta = \left(\frac{\delta_0 - \delta_{HA}}{\delta_0}\right) \times 100 \tag{4}$$

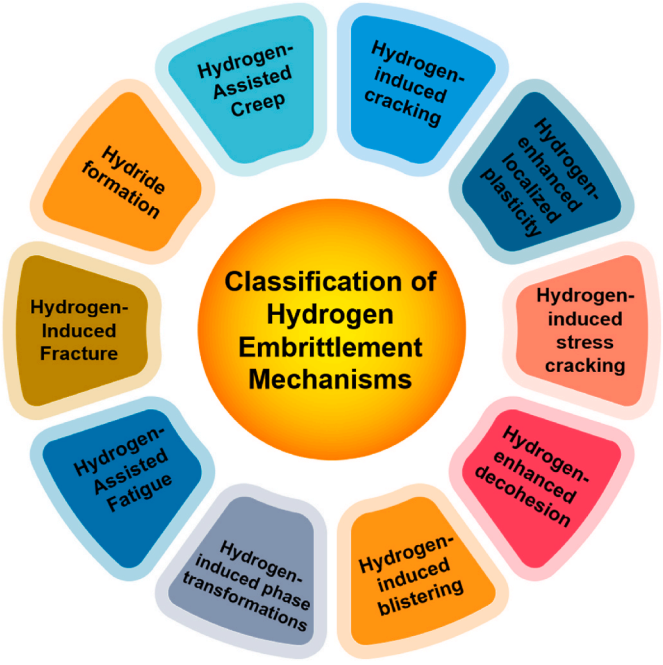

Fig. 4. Classification of HE mechanisms.

$$\Delta\sigma = \left(\frac{\sigma_0 - \sigma_{HA}}{\sigma_0}\right) \times 100 \tag{5}$$

Where, δ_0 and δ_{HA} are the elongation values obtained from quasi-static tensile tests conducted under non-hydrogen-charged and hydrogen-charged conditions, respectively. σ_0 and δ_{HA} represent the corresponding ultimate tensile strengths under the same testing conditions. Hydrogen-induced cracking (HIC) for example can be evaluated using quantitative parameters such as crack length ratio (CLR), crack thickness ratio (CTR), and crack sensitivity ratio (CSR) (refer to Eqs. (6)–(8)) [63]. CLR is the ratio of the total crack length ($\sum a$) to the specimen width (W), indicating surface crack distribution. CTR is the ratio of total crack depth ($\sum b$) to specimen thickness (t), reflecting through-thickness propagation. CSR quantifies the relative impact of cracks by calculating the combined effect of their length and depth, normalized against the specimen's total cross-sectional area.

$$\mathrm{CLR} = \frac{\sum a}{W} \times 100\% \tag{6}$$

$$\mathrm{CTR} = \frac{\sum b}{t} \times 100\% \tag{7}$$

$$\mathrm{CSR} = \frac{\sum (a \times b)}{W \times t} \times 100\% \tag{8}$$

3.4. Comparison of HE in different material types

HE impacts metals, composites, and polymers differently due to their distinct structures and material properties. Metals; especially high-strength steels, titanium, and aluminum alloys are most vulnerable, as HAs readily diffuse into their microstructure, interacting with grain boundaries, dislocations, and defects, leading to embrittlement through mechanisms like HIC, HELP, and HISC [24,96]. Composites, which combine a matrix (often polymeric or metallic) with reinforcing fibers like carbon or glass, are generally more resistant; however, hydrogen can still degrade the matrix or cause fiber-matrix delamination, reducing overall strength [97–99]. Polymers are less prone to embrittlement but can still suffer from hydrogen-induced effects such as swelling,

Table 2
Overview of hydrogen-related damage mechanisms, material susceptibility, environmental influences, and mitigation approaches.

Mechanisms	Materials Affected	Environmental Conditions	Mitigation
HIC: HIC occurs when hydrogen atoms diffuse into a material and accumulate at internal defects like grain boundaries (GBs), or non-metallic (e.g., sulfur), causing crack initiation and growth [60]. 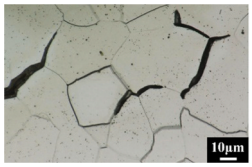	▪ Pure iron ▪ Low-to medium strength steels [61]	▪ Mostly found in sour environments, such as those containing hydrogen sulfide (H_2S). ▪ HIC can develop even without residual or applied tensile stress [62].	▪ Reducing the amount, the size, and the volume fraction of inclusions decreases the material susceptibility to HIC [63].
HELP: Hydrogen enhances dislocation mobility, leading to localized plastic deformation and reduced ductility [64].	▪ Ferritic, martensitic, and austenitic steels, iron, nickel, and zirconium alloys [64,65]	▪ High hydrogen fugacity environments (e.g., high-pressure H_2 gas). ▪ Applied or residual stress accelerates HELP [66,67].	▪ Lowering hydrogen exposure through coatings or inhibitors.
HISC: This mechanism occurs primarily near the surface of a material due to the diffusion and accumulation of hydrogen under stress. It is characterized by surface-initiated cracks that are typically isolated, larger near the surface, and decrease in size and number toward the material's interior. 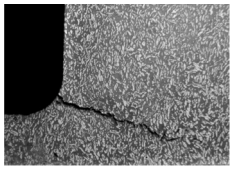	▪ Duplex and supermartensitic stainless steels [68]	HISC occurs due to the combination of three conditions: • Tensile stress • A susceptible microstructure • A hydrogen source (e.g., cathodic protection systems, subsea equipment)	▪ The risk of HISC can be reduced by maintaining austenite spacing below 30 μm [69].
HEDE: When hydrogen atoms accumulate in the metal lattice, they reduce the cohesive energy between atoms, lowering the energy needed to crack the crystal along GBs, crystallographic planes, or phase interfaces.	▪ High-Mn and high-Al steel ▪ Nickel superalloys ▪ Titanium alloys ▪ Ni-based alloys [70–73].	▪ Higher hydrogen concentrations and material strength levels [74]	▪ Use of hydrogen-resistant elements (e.g., boron, molybdenum, tungsten)
HIB: In this mechanism, HAs diffuse into a material and accumulates at specific locations (e.g., microvoids and internal cracks), forming pockets of hydrogen gas, known as blisters [75]. These gas pockets create internal pressure, causing the material's surface to bulge or blister ss shown in the figure. 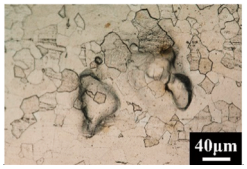	Ferrous (e.g., pure iron, AISI 304 and 430 AISI stainless steel) & non-ferrous (e.g., 1100 Al, α-brass, Ni) materials [76].	▪ Larger current densities and longer charging times	▪ Inclusion control and coatings [77]
HF: Hydrogen reacts with certain metals (e.g., Ti, Zr, V) to form brittle hydride phases, which can lead to crack initiation and catastrophic failure under stress.	▪ Titanium alloys ▪ Zirconium alloys ▪ Vanadium alloys [78]	▪ High temperature, stress, and hydrogen-rich environments	▪ Use of hydride-resistant alloys ▪ Heat treatments [79]
HAF: HAF is a hydrogen-related damage mechanism where hydrogen atoms, absorbed from corrosive environments or high-pressure gas, weaken a material's structure and accelerate fatigue crack growth under cyclic loading.	▪ Carbon steels ▪ Stainless steels ▪ Nickel alloys [80–82]	▪ Hydrogen Source + Cyclic Loading	▪ Increasing the density of microstructural traps [83]
HIF: A brittle fracture mechanism where hydrogen reduces fracture toughness, leading to sudden failure under stress.	▪ High strength steels ▪ Aluminium alloy ▪ Titanium alloys [84–86]	▪ High hydrogen fugacity ▪ active corrosion with damaged paint	▪ Hydrogen Barrier Coatings ▪ Avoiding high-stress concentration [87]
HAC: In this mechanism, the presence of hydrogen accelerates the time-dependent deformation, or creep, of a material under stress, particularly at elevated temperatures.	▪ α-Fe ▪ Ni-Cr-Fe alloys [88,89]	▪ High-temperature hydrogen environments ▪ Significantly affected by the levels of creep stress	▪ Lower service temperatures and stresses
HIPT: HIPT is a form of hydrogen damage mechanism where hydrogen alters the phase stability of a material, resulting in the creation of brittle phases or changes in the microstructure that reduce its mechanical strength [90].	▪ Stainless steels ▪ Titanium alloys ▪ Zirconium alloys [91–93]	▪ High hydrogen concentrations	▪ Annealing in air [94]

softening, or degradation of polymer chains, particularly under high-pressure or high-temperature conditions [100]. While metals face the most severe consequences, HE can still compromise the structural integrity of composites and polymers in hydrogen-rich environments.

In plain carbon steel, HE typically results from hydrogen diffusion into the metal, accumulating at GBs and defects, which leads to crack initiation and growth [101]. Carbon compounds like carbides can trap hydrogen, intensifying this effect and further weakening the material [102]. Stainless steels, despite their corrosion resistance, are still susceptible; especially high strength grades; as hydrogen reduces ductility and promotes stress corrosion cracking at GBs [103]. Aluminum and its alloys are generally more resistant to HE, but under high hydrogen pressures, hydrogen absorption can still cause hydride formation, leading to brittleness and cracking; particularly in copper- or magnesium-containing alloys [61,62,104]. Copper alloys show good resistance under normal conditions, though elevated hydrogen pressures can still cause embrittlement via hydride formation, reducing ductility and toughness [105]. Nickel-based alloys are highly resistant to HE due to their stable microstructure, but in high-strength, high-stress conditions, they can still suffer from crack initiation, especially at GBs or due to hydrides under extreme hydrogen exposure [106,107]. Titanium and its alloys offer superior HE resistance through a protective oxide layer that limits hydrogen uptake, yet they are still vulnerable under high hydrogen concentrations and temperatures, where brittle titanium hydrides can form and degrade mechanical properties [108–110]. Across all these materials, HE susceptibility varies with alloy composition, microstructure, and environmental factors, requiring careful material selection, processing control, and protective strategies to mitigate failure risks in hydrogen storage applications.

4. Hydrogen storage tank materials and their susceptibility to HE

Hydrogen storage plays a vital role in industries such as fuel cell technology, where metallic tanks—commonly made from steel, aluminum, titanium, and nickel-based alloys—are used due to their strength and durability [111]. Each material offers specific benefits and drawbacks. Steel is cost-effective and strong, suitable for low to medium-pressure applications, but is heavy and prone to HE, requiring monitoring [112,113]. Stainless steel improves corrosion resistance for higher pressures [114]. Aluminum is lightweight and more resistant to HE than steel, making it ideal for mobile uses like vehicles, though its lower strength limits high-pressure applications unless reinforced [115]. Titanium combines high strength, corrosion resistance, and HE resistance, ideal for aerospace, but its high cost restricts widespread use [116]. Nickel-based alloys are suited for cryogenic or high-pressure environments due to their superior corrosion and temperature resistance, though they are costly [26]. Material choice depends on pressure requirements, weight, environment, and budget. Crucially, a material's microstructure and alloy composition heavily influence HE susceptibility; affecting how hydrogen interacts with the metal, promoting brittleness and cracking. Understanding these properties is essential for selecting safe, long-lasting materials for hydrogen storage.

4.1. Microstructure influence

The microstructure of a material refers to the arrangement of its grains, phases, and defects at the microscopic level. HE is closely linked to how hydrogen interacts with these features, as they can act as sites for hydrogen accumulation, leading to crack formation and propagation. The microstructure may affect HE susceptibility by the following ways.

a) **Grain Boundaries (GBs):** Hydrogen tends to accumulate at GBs, which are the interfaces between individual crystals in a material. If these boundaries are weak or poorly bonded, they become preferential sites for hydrogen to enter, leading to increased brittleness. Materials with finer grains typically have more GBs, which can increase the risk of HE unless the GBs are well-bonded or resistant to hydrogen penetration.

GBs play a critical role in HE across various metallic materials, as evidenced by multiple studies. Liu et al. [117] demonstrated that in magnesium, hydrogen preferentially segregates at high-energy GBs, reducing the critical energy release rate and promoting brittle fracture, especially in boundaries with higher misorientation. Mai et al. [107] found a similar trend in nickel, where high-energy, random GBs exhibited significant hydrogen segregation and reduced cohesion, while low-energy, coherent GBs showed minimal weakening. Their work emphasized that increasing the proportion of special GBs can mitigate HEDE effects. Momida et al. [118] expanded on this by showing that hydrogen-vacancy complexes at GBs in α-iron drastically reduce tensile strength, contributing to delayed but severe brittle failure. GBE emerges as a practical solution to these vulnerabilities. Bechtle et al. [119] increased special GBs in nickel through thermomechanical processing, which nearly doubled ductility and improved fracture toughness under hydrogen exposure. Similarly, Taji et al. [120] showed that in Alloy 725, the GB microstructure influenced crack propagation, with over-aged samples showing more severe HE due to less favorable GB character. Xi et al. [121] further confirmed that optimizing GB types; such as increasing special or low-angle boundaries through alloying (e.g., with 1 % Cu); can enhance hydrogen trapping and reduce diffusion, thereby improving HE resistance. Collectively, these studies underscore the critical influence of GB character and distribution on HE behavior and point toward GB engineering (GBE) as a key strategy in designing hydrogen-resistant materials, especially for welded components in hydrogen storage systems.

Thus, GBs play a critical role in HE across various materials. Hydrogen accumulates at high-energy, poorly bonded GBs, leading to increased brittleness and reduced material strength. Strategies such as enhancing the fraction of special low-energy GBs, grain-boundary engineering, and optimizing microstructures can significantly mitigate the effects of hydrogen, improving the material's resistance to embrittlement. These findings highlight the importance of GB characteristics in controlling HE and offer promising approaches for designing more resilient materials.

b) **Phase Composition:** Many alloys contain different phases, such as martensite, ferrite, or austenite. The presence of certain phases, particularly martensitic structures, can make materials more susceptible to HE. This is because these phases often have high dislocation densities, which can facilitate hydrogen entry and crack initiation. On the other hand, phases with a more stable atomic structure may be less prone to HE.

Recent research has significantly advanced the understanding of HE in complex microstructures, particularly in multiphase steels and high-performance alloys. Manda et al. [122] showed that in ferrite-martensite dual-phase (DP) steels, hydrogen promotes strain localization in ferrite and damage at ferrite-martensite interfaces, with hydrogen accumulation enhanced by high phase boundary densities and lower martensite tetragonality. Their model, combining interface dislocation pile-ups and void nucleation, offers an alternative to traditional HEDE explanations. Li et al. [123] used cross-scale simulations to reveal that HE sensitivity in chromium alloy steels peaks at 5–8 % Cr, due to hydrogen trapping in chromium carbides and enrichment at phase boundaries, which drives crack growth. Örnek et al. [124] emphasized real-time HE analysis in duplex stainless steels, revealing that hydrogen destabilizes the microstructure through phase decomposition, especially in austenite, challenging conventional views of HE as purely due to lattice decohesion. Wang et al. [125] addressed HE in aluminum alloys, showing that transforming nanoprecipitates from the η phase to the T phase significantly reduces crack formation by trapping

hydrogen at defects, offering a pathway to improve alloy durability without changing overall composition. Dong et al. [126] demonstrated that increased phosphorus content in DP steels heightens HE susceptibility by promoting HIC in martensite and interfaces, with ductility loss attributed to mechanisms such as HESIV, HEDE, and HELP. Collectively, these studies highlight the complex, microstructure-dependent nature of HE and reinforce the importance of phase design, alloying strategies, and real-time monitoring in mitigating hydrogen-induced failure in structural materials.

Thus, phase composition significantly influences HE in alloys. Phases with high dislocation densities, such as martensite, are more susceptible to HE, as they promote hydrogen entry and crack initiation. Research shows that phase boundaries, such as ferrite-martensite interfaces, and hydrogen enrichment at these boundaries play a key role in embrittlement. Strategies to optimize phase composition and design alloys with stable, hydrogen-resistant phases can help mitigate the risk of HE and improve material durability.

c) **Dislocations and Defects:** Dislocations, vacancies, and other crystal defects can act as hydrogen trapping sites. Materials with a higher density of dislocations or vacancies tend to trap more hydrogen, making them more vulnerable to embrittlement. This is particularly significant in high-strength materials, which often have more dislocations due to their processing.

Recent studies have deepened the understanding of how dislocations, vacancies, and hydrogen interactions contribute to HE, especially in austenitic stainless steels. Ye et al. [127] found that increasing hydrogen concentration in 316SS reduced tensile strength and ductility, promoted martensite formation through hydrogen-induced lattice expansion, and caused a shift in fracture morphology from ductile to brittle. Their work, supported by XRD, PAS, and TDS, highlighted the persistence of dislocations and vacancy recovery with annealing. Ye et al. [128] further emphasized that traditional techniques like TDS provide limited insights into hydrogen–defect interactions, recommending internal friction (IF) as a more sensitive method to study dislocation dynamics and vacancy–hydrogen complexes. Sugiyama et al. [129] used low-temperature TDS to show that hydrogen enhances vacancy formation but not dislocation density in pure iron under plastic strain, with defects localizing near grain boundaries. Chiari et al. [130] used positron annihilation lifetime spectroscopy to identify vacancy-hydrogen agglomerates as precursors to embrittlement in 304 stainless steel, noting that stress facilitated hydrogen diffusion and vacancy clustering even after surface hydrogen removal. Collectively, these studies highlight that hydrogen-induced degradation in steels is closely tied to microstructural defects, especially dislocation-vacancy interactions, which influence crack initiation and material embrittlement, particularly under stress or thermal exposure.

Thus, dislocations, vacancies, and other defects play a crucial role in HE by acting as hydrogen trapping sites. Materials with higher defect densities, such as those with more dislocations, are more susceptible to HE. Studies on various steels and alloys highlight how hydrogen interacts with dislocations and vacancies, leading to increased brittleness and changes in fracture morphology. Understanding these interactions and utilizing techniques like IF and positron annihilation spectroscopy can provide deeper insights into the mechanisms behind HE.

d) **Hydride Formation:** In some alloys, particularly those with elements like titanium, nickel, and aluminum, hydrogen can react with the metal to form brittle hydrides. These hydrides can significantly weaken the material, especially at high hydrogen concentrations, and may initiate crack propagation.

Ongoing investigations have significantly advanced the understanding of HE in Ti-6Al-4V alloys, especially regarding the influence of microstructure, hydrogen concentration, and manufacturing methods. Deconinck et al. [131] showed that L-PBF-processed Ti-6Al-4V, particularly in the as-built martensitic α' state, is highly susceptible to HE due to stress-induced hydride formation (SIHF) and the interaction of hydrogen with porosity, which promotes early crack initiation. At high strain rates, the failure was dominated by the HELP mechanism, while SIHF played a greater role at low strain rates. Nguyen et al. [132] further clarified the effect of hydrogen phase state, demonstrating that solute hydrogen (SH) mainly induced intergranular void formation, while hydride phases (HP) led to more severe two-layer brittle fractures. Increasing hydrogen concentration worsened the loss of ductility, especially in total elongation. Deconinck et al. [133] also highlighted how L-PBF process parameters affect HE susceptibility: polished surfaces reduced hydrogen uptake, while building orientation influenced hydrogen distribution via β GB alignment. Zhang et al. [134] detailed a three-stage hydride formation process—beginning with hydrogen diffusion into the β phase, followed by hydride nucleation at α/β interfaces, and ending with uniform hydride distribution in the α phase. This evolution shifted fracture modes from ductile dimpling to mixed brittle modes. Collectively, these studies underline that HE in Ti-6Al-4V is governed by complex interactions between hydrogen, microstructure (especially β phase and porosity), and mechanical stress, emphasizing the need for microstructural optimization and surface quality control to improve performance in hydrogen-rich environments.

Thus, hydride formation significantly contributes to HE in alloys, particularly those containing elements like titanium. The formation of brittle hydrides, especially at high hydrogen concentrations, weakens the material and promotes crack initiation and propagation. Studies on Ti-6Al-4V reveal how different microstructures and hydrogen concentrations affect the formation of hydrides and the resulting embrittlement, emphasizing the need for careful control of processing parameters to minimize hydrogen-induced damage and improve material performance in hydrogen-rich environments.

Table 3 summarizes the influence of various microstructural features on the susceptibility of materials to HE. GBs, particularly high-energy and poorly bonded ones, serve as favorable sites for hydrogen accumulation, leading to increased brittleness. Conversely, special low-energy GBs and GBE techniques have been shown to improve resistance to HE. Phase composition also plays a critical role; for instance, martensitic structures and phase interfaces can facilitate hydrogen trapping and crack propagation, whereas phase transformations and stable austenitic structures may help mitigate HE. Dislocations and defects, including vacancies, act as hydrogen traps and promote crack initiation, thus accelerating embrittlement, especially under stress-assisted conditions. Furthermore, hydrogen-induced hydride formation contributes to embrittlement by initiating cracks and reducing ductility. The nature and morphology of the hydrides, as well as surface characteristics and grain alignment, significantly affect hydrogen uptake and fracture behavior. Collectively, these findings highlight the complex interplay between microstructural attributes and hydrogen behavior, emphasizing the need for microstructural control to enhance material resistance to HE.

4.2. *Alloy composition influence*

The composition of the alloy, the elements added to a base metal like steel or aluminum, plays a crucial role in determining a material's susceptibility to HE [135]. Various alloying elements can either exacerbate or reduce the effects of HE, influencing the material's behavior in hydrogen environments. Carbon content significantly influences HE in steels [136]. While enhancing strength, higher carbon levels can increase susceptibility to embrittlement, especially under elevated hydrogen pressures. Carbon can form carbides that interact with hydrogen, potentially leading to cracking and weakening of the material.

Kim et al. [137] investigated the HE behavior of austenitic stainless steels with 0.1–0.3 wt% carbon. They found that increasing carbon

Table 3
Summary of microstructural influences on HE.

Microstructural Feature	Effect on HE	Key Findings	Ref.
Grain Boundaries (GBs)	Act as hydrogen accumulation sites, especially high-energy GBs; increase brittleness if poorly bonded	- High-energy GBs in Mg and Ni promote brittle fracture - Special/low-energy GBs reduce HE sensitivity - GBE improves ductility and toughness - Alloying (e.g., Cu) enhances hydrogen trapping	[107, 117–121]
Phase Composition	Certain phases (e.g., martensite) with high dislocation densities promote hydrogen entry and cracking	- Ferrite-martensite interfaces enhance H accumulation - Cr-carbides and phase boundaries drive cracking - Phase decomposition in austenite destabilizes microstructure - Phase transformation reduces crack initiation	[122–126]
Dislocations and Defects	Dislocations, vacancies act as H-trapping sites; facilitate crack initiation and reduce ductility	- Hydrogen induces martensite formation and fracture mode shift - IF spectroscopy better captures H–defect interactions - H enhances vacancy formation near GBs - Stress aids hydrogen-vacancy clustering	[127–130]
Hydride Formation	Hydrogen reacts with metals to form brittle hydrides; leads to crack initiation and reduced ductility	- L-PBF Ti-6Al-4V prone to SIHF and HELP - Hydride vs. SH fracture modes differ - Surface finish and β grain alignment affect H uptake - Three-stage hydride formation alters fracture mechanism	[131–134]

content reduced hydrogen-induced degradation of tensile properties but had little effect on hydrogen diffusivity. Cracks initiated at GBs, where hydrogen concentration was highest, but carbon delayed initiation by strengthening these boundaries. Crack propagation occurred through α' and ε martensites inside grains but was halted at GBs, preventing deep penetration. Carbon stabilized austenite, which prevented martensite formation and crack propagation, improving ductility and reducing elongation loss due to HE. Liu et al. [138] studied HE in structural steels essential for the hydrogen economy. They compared a steel with titanium carbides (TiCs) and another with molybdenum (Mo), which forms Ti-Mo carbides with more carbon vacancies. Their results showed that Mo increases the hydrogen trapping capacity by enabling hydrogen to access carbon vacancy traps in the carbides. Pichler et al. [136] studied how pearlite influences HE in ultra-low carbon ferritic steels. They found that the Fe-0.02C alloy was highly sensitive to HE, while Fe and Fe-0.1C alloys showed less sensitivity. The presence of high-angle GBs (HAGBs) in the Fe-0.1C alloy trapped hydrogen, reducing its diffusivity and making it less likely for critical hydrogen levels to accumulate. This reduced the occurrence of crack initiation and propagation compared to Fe-0.02C, which exhibited more hydrogen-related cracks. Pinson et al. [139] investigated the role of cementite, an iron carbide, in HE in martensitic steels with similar dislocation densities but differing cementite concentrations. They found that cementite effectively traps hydrogen, reducing hydrogen diffusion and increasing resistance to HE by preventing hydrogen from reaching critical microstructural sites. However, when the steel samples were fully saturated with hydrogen before testing, cementite lost its influence, and fracture propagation was controlled by HAGBs, highlighting the significance of dislocation density and the carbide's role in the HE mechanisms. Rodoni et al. [140] investigated the hydrogen transport properties and HE resistance of DP ferritic-martensitic low alloy steels (LASs), with control conditions including ferritic-pearlitic and fully martensitic microstructures. The study showed that tempering DP-LAS decreased hardness and enhanced carbide precipitation, leading to higher hydrogen diffusion coefficients and reduced hydrogen trapping, primarily due to dislocation annihilation. Additionally, an increase in martensite content reduced the hydrogen diffusion coefficient, with the martensite carbon content playing a secondary role in controlling hydrogen diffusion. In slow strain rate tests, DP-LAS with about 50 % tempered martensite exhibited the highest resistance to HE, offering valuable insights for designing DP-LASs for hydrogen-related applications. Noh et al. [141] explored the impact of carbon on HE in stable austenitic stainless steels by adding 0.02 wt% and 0.1 wt% C. During deformation, both steels showed planar slip and fine dislocation structures, followed by mechanical twinning. However, after hydrogen pre-charging, the alloy with higher carbon (0.1 wt%) demonstrated greater susceptibility to HE. The study suggested that carbon enhances planar slip and refines mechanical twins, which leads to more sites for stress concentration and hydrogen trapping, accelerating embrittlement. High resistance to HE was attributed to stable austenite and shallow hydrogen diffusion depths, while the higher carbon content resulted in more intersections of dislocation walls, twins, and GBs, increasing sites for hydrogen trapping and crack formation. The findings emphasized that austenite stability alone is not sufficient for hydrogen resistance, and the deformation mechanism also plays a crucial role in the design of austenitic stainless steels for hydrogen applications.

Chromium improves corrosion resistance in stainless steels but can increase GB susceptibility to hydrogen attack, while nickel enhances toughness and stabilizes microstructures, though excessive amounts may raise HE risk. Li et al. [123] showed that Cr carbides ($Cr_{23}C_6$, Cr_7C_3, Cr_3C_2) trap hydrogen more than the iron matrix, with peak HE sensitivity at 5–8 % Cr. Symons [142] found that increasing Cr improved ductility in uncharged Ni-Cr-Fe alloys, but under hydrogen, high Cr content led to brittle intergranular fracture due to reduced stacking-fault energy and increased slip planarity. Simonetti et al. [143] reported that hydrogen–vacancy clusters and weakened Cr-related bonds in Fe–Cr–Ni alloys promote crack initiation and stress corrosion. Rodoni et al. [144] showed that raising Ni to 3 wt% in low alloy steels reduced hydrogen diffusion and increased trapping without harming HE resistance, suggesting possible revision of ASME B31.12 limits. Balytskyi et al. [145] observed that at 293 K, HE decreased with Ni content up to 23 wt%, but higher Ni led to embrittlement, especially at 973 K. Thermomechanical treatment improved plasticity and performance in hydrogen environments.

Molybdenum and vanadium improve steel strength and hardness but can increase HE susceptibility at high concentrations by forming brittle phases. Liu et al. [146] found that VMo phases had lower hydrogen solubility than VW phases, enhancing HE resistance. W and Mo concentrations above 0.1875 improved V membrane HE resistance, while lower concentrations weakened its solid-solution strengthening. Peral et al. [147] showed that V-added steel, with strong hydrogen-trapping molybdenum–vanadium nanometric carbides, had lower hydrogen diffusion and embrittlement compared to V-free steel, which had weaker traps. Lee et al. [148] investigated the effects of Cr, V, and Mo carbides in tempered martensitic steel, finding that V carbides provided good HE resistance, but Mo carbides were the most effective, suppressing hydrogen penetration and minimizing strength loss.

Titanium alloys, favored for hydrogen storage due to their corrosion resistance and low HE susceptibility, face challenges from hydride formation in hydrogen-rich environments. Briant et al. [149] found that grade 2 titanium was resistant to hydrogen cracking in acidic saltwater

but became brittle in gaseous hydrogen at high temperatures due to hydride formation. Grade 3 titanium, with higher iron content, showed susceptibility to HE, as iron facilitated hydride nucleation. Shih et al. [150] observed two fracture mechanisms in Ti-4 wt% Al alloy under hydrogen: plastic deformation and brittle fracture due to stress-induced titanium hydride at crack tips. Wu et al. [151] found that hydride properties in titanium changed at 423 K, with a transition from octahedral to tetrahedral hydrogen sites, enhancing mechanical properties and offering insights into hydrogen-induced embrittlement.

Similarly, in aluminum alloys, elements like copper, magnesium, and silicon are often added to enhance strength, but they may increase susceptibility to HE by promoting the formation of brittle phases, such as aluminum hydride or intermetallic compounds [152]. The presence of these elements requires careful control of alloy composition to balance the material's strength and resistance to hydrogen-induced damage [153].

Thus, the alloy composition significantly influences the susceptibility of materials to HE as shown in Fig. 5. Elements like carbon, chromium, nickel, molybdenum, and vanadium in steels play pivotal roles in either exacerbating or reducing HE, based on their interactions with hydrogen and their effects on microstructural features. Carbon, while enhancing strength, increases vulnerability to HE by promoting the formation of carbides that can lead to cracking. Chromium can improve corrosion resistance but also increase the material's susceptibility to hydrogen attack at GBs. Nickel, known for enhancing strength and toughness, can reduce HE by stabilizing the microstructure, though excessive amounts may still promote embrittlement. Molybdenum and vanadium, when present in appropriate amounts, help improve hydrogen resistance by trapping hydrogen and reducing its diffusion, but excessive concentrations can lead to the formation of brittle phases. In titanium alloys, the primary challenge comes from hydride formation in hydrogen-rich environments, which can cause embrittlement, although careful control of alloy composition and processing methods can mitigate this risk. Similarly, aluminum alloys, while benefiting from enhanced strength due to elements like copper, magnesium, and silicon, are prone to HE due to the formation of brittle phases. Therefore, optimizing alloy compositions is crucial to balancing the material's mechanical properties with its resistance to hydrogen-induced damage, making it essential for applications in hydrogen storage.

5. Factors influencing HE in welded regions of hydrogen storage tanks

Welding joints are commonly used in the construction of HSTs, especially to join the various components such as the tank's shell, nozzles, and fittings. However, the use of welding in these tanks requires careful consideration due to the unique challenges posed by hydrogen, particularly HE and the risk of corrosion. Welding creates a fusion between metal parts, and in the case of HSTs, these joints are critical for maintaining the integrity of the tank under high-pressure conditions. Metals like steel and aluminum, which are commonly used in hydrogen tanks, are particularly vulnerable to this phenomenon, especially in high-stress or high-pressure environments. As a result, welding procedures must be carefully controlled to avoid introducing hydrogen into the material. Special welding electrodes, preheating of the material, and moisture control during welding are necessary to mitigate the risk of embrittlement and ensure the strength and durability of the welds. Additionally, the choice of material is crucial when welding HSTs. Materials used for the welding process must be resistant to HE and corrosion, which are common issues in hydrogen environments. Stainless steel and aluminum alloys are often preferred for their ability to resist these issues. For tanks made of composite materials, such as Type II and Type III tanks, welding is typically used only for the metal liner, while the composite overwrap is bonded using other methods like adhesive bonding or filament winding. The welding process itself also needs to be carefully managed. Techniques such as Tungsten Inert Gas (TIG) welding or Metal Inert Gas (MIG) welding are typically used in the construction of HSTs because they provide strong, clean joints that minimize defects. Any flaws in the weld could lead to leakage or failure of the tank under pressure. To ensure the integrity of the welded joints, non-destructive testing methods such as ultrasonic testing, X-ray inspection, and hydrogen leak detection are often employed to detect any potential weaknesses that could compromise the safety of the tank. Another concern with welding is the creation of heat-affected zones (HAZ) around the weld. These areas, which experience a temperature change during the welding process, can alter the metal's properties, making it more susceptible to embrittlement or corrosion. In HSTs, these zones must be carefully controlled to ensure that they do not weaken the structure or lead to failure. In some cases, post-weld heat treatments or surface coatings are used to restore the material's strength and prevent further degradation. HE in the welded regions of HSTs is influenced by several key factors. Material composition plays a crucial role, as alloys prone to forming brittle phases are more susceptible to HE. The welding process itself can introduce residual stresses and thermal effects that alter the microstructure, making the heat-affected zone (HAZ) more vulnerable to embrittlement. Defects such as porosity or cracks in the weld can act as stress concentrators, facilitating hydrogen absorption and crack propagation. The extent of hydrogen exposure, temperature conditions, and strain rates also affect the material's resistance to HE, with higher hydrogen concentrations accelerating the process.

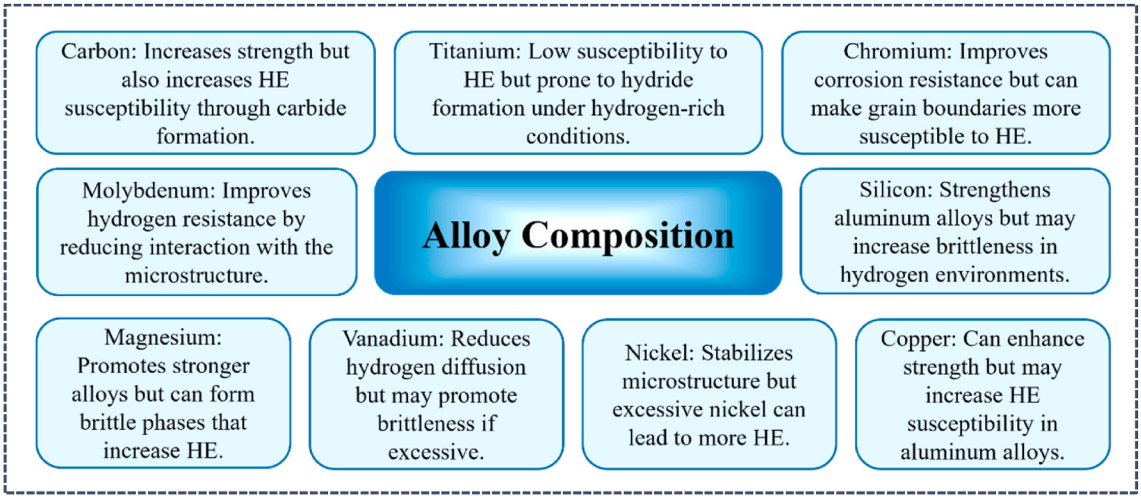

Fig. 5. Impact of alloy composition on HE susceptibility in materials.

Additionally, fine grain structures and grain boundary characteristics influence the tank's ability to resist hydrogen-induced damage. Proper material selection, welding techniques, and post-weld treatments are critical to mitigating the risk of HE in welded regions. Table 4 compiles a selection of significant research efforts that collectively dissect the main contributors to HE sensitivity in welded zones. These works span several key domains: alloying element effects, the influence of welding parameters, the role of post-weld heat treatment, residual stress implications, and the impact of weld-related defects. For each study, the table outlines the research objective, the specific properties or characteristics examined, and a summary of the core findings.

6. Mitigation strategies and protective measures

HE in the welded regions of hydrogen tanks and vessels can significantly degrade the material's integrity, posing serious safety risks. To reduce the risk of HE in hydrogen storage tank materials, engineers focus on optimizing both microstructure and alloy composition [162]. Some of the key strategies employed include grain refinement, alloying elements selection, heat treatments, and the use of hydrogen diffusion barriers [163] as summarized in Fig. 6.

6.1. Grain refinement

Grain refinement is one such strategy, where finer grains are introduced to improve the strength and toughness of the material. While smaller grains enhance mechanical properties, care must be taken to balance this with the potential for embrittlement at GBs. If the GBs become too brittle, they may act as sites for crack initiation under hydrogen exposure. Therefore, it's essential to achieve an optimal grain size that enhances strength without compromising toughness. Fan et al. [164] studied the effect of grain size (4–12 μm) on HE in 304 austenitic stainless steel (ASS). They found that HE resistance increased with grain refinement, as it reduced strain localization, which acts as a pathway for hydrogen diffusion and crack initiation. The study revealed that grain size did not affect strain-induced martensite (SIM) transformation during hydrogen-charged SSRT, suggesting that SIM formation was not responsible for the observed differences in HE resistance. They also observed that hydrogen diffusion in 304 ASS was influenced by a competition between short-circuit diffusion along random GBs and hydrogen trapping at dislocations, with the highest hydrogen diffusion coefficient occurring at an 8 μm grain size. Additionally, HIF transitioned from a dimple fracture to a mix of quasi-cleavage and dimple fracture as grain size decreased. Mine et al. [165] studied the effect of ultrafine grain refinement on HE in metastable austenitic type 304 steel by performing micro-tensile tests on high-pressure-torsion-processed specimens with grain sizes ranging from 0.1 to 0.5 μm. The results showed that specimens with average grain sizes below ~0.4 μm exhibited limited uniform elongation, followed by a steady-stress regime, attributed to martensitic transformation. The ultrafine-grained specimens with ~0.5 μm grain size achieved high yield stress and moderate elongation in the uncharged state. The Hall–Petch relationship was maintained for both uncharged and hydrogen-charged specimens, with hydrogen charging increasing the friction stress by 40 % without altering the Hall–Petch coefficient. Hydrogen-induced ductility loss was mitigated by ultrafine grain refinement, primarily affecting local deformation post-martensitic transformation rather than the transformation itself. Khalid et al. [166] explored the effect of grain size and precipitation on hydrogen uptake and HE susceptibility in alloy 718. Their results showed that fine-grained microstructures, produced by friction-stir processing (FSP), absorbed more hydrogen compared to coarse-grained solution-treated (ST) conditions, due to the increased trapping of hydrogen at GBs and dislocations. However, the presence of γ' and γ'' phases reduced hydrogen uptake, suggesting these phases have a low affinity for hydrogen. Despite absorbing more hydrogen, the fine-grained FSP microstructure exhibited similar or reduced susceptibility to HE compared to the coarse-grained ST condition. Furthermore, the FSP-A condition (fine-grained and aged) showed significantly lower HE susceptibility than the peak-aged (PA) condition. The study also found that hydrogen increased surface hardness, particularly in the ST condition, and that the fine-grained FSP and FSP-A microstructures inherently demonstrated higher resistance to HICthan their coarse-grained counterparts. The authors propose that future work should focus on understanding the relationship between crack initiation and propagation in fine-grained alloy 718.

6.2. Grain boundary engineering (GBE)

Grain boundary engineering (GBE) is a technique used to mitigate HE by manipulating the GBs of a material to enhance its resistance to hydrogen-induced cracking. This process involves altering the misorientation of grains to favor “special" GBs, which are more resistant to hydrogen diffusion and less prone to fracture under stress. By optimizing grain boundary characteristics through heat treatments or severe plastic deformation, GBE improves the material's toughness, reduces hydrogen penetration, and increases its overall resistance to embrittlement in hydrogen-rich environments. Kwon et al. [167] investigated the enhancement of HE resistance in Fe-17Mn-0.8C (wt%) TWIP steels using a GBE approach. The study compared the HE resistance of GBE-treated TWIP steels with Al-added variants (Fe-17Mn-0.8C-1Al and Fe-17Mn-0.8C-2Al). Through GBE, the fraction of special boundaries, which share a high fraction of lattice points between neighboring grains, increased from 48 % to 59 %, and GBs adopted a more ragged morphology. After hydrogen charging, all samples exhibited a transition from ductile dimple fracture to brittle intergranular fracture, with the alloys containing higher fractions of special boundaries showing greater resistance to hydrogen-induced embrittlement. Notably, the HE resistance of the GBE-treated steels was improved to a level comparable to that of the Al-added TWIP steels. The enhancement in resistance was attributed to both the increased fraction of special boundaries and the loss of continuity in random boundaries. This work highlights the potential of controlling grain boundary character distributions to significantly enhance HE resistance without the need for alloying additions like aluminum. In another study, Kwon et al. [168] studied the effect of strain rate ($10-3 \leq \leq 10-5\ s^{-1}$) on HE in Fe−17Mn−0.8C TWIP steel. Two types of specimens were tested: hot-rolled (AR) and those processed by GBE. For AR samples, fracture strength and ductility decreased with lower strain rates due to hydrogen accumulation near crack tips. In contrast, GBE samples exhibited minimal loss in fracture strength and ductility, as special GBs inhibited hydrogen-induced crack initiation and propagation. Sun et al. [169] investigated the HE sensitivity of high-purity nickel with different grain boundary characteristics. One sample had straighter GBs, while the other had more rugged boundaries. Hydrogen testing showed the sample with more rugged boundaries had a higher HE index. The study found that while special GBs (e.g., twin boundaries) had a small effect on HE resistance, increasing grain boundary curviness significantly improved resistance. The sample with more curved boundaries showed less ductility loss and more ductile fracture, suggesting that grain boundary curviness plays a crucial role in enhancing HE resistance.

6.3. Alloying elements

The selection of appropriate alloying elements is another critical approach. Certain elements can be added to the base material to enhance resistance to hydrogen diffusion, mitigate the formation of brittle phases, and improve the overall toughness of the material. Alloying elements such as chromium, nickel, and molybdenum can be particularly effective in improving resistance to hydrogen-related damage. By carefully choosing these elements, engineers can improve the material's overall durability and minimize the risk of embrittlement in hydrogen environments. Zhang et al. [170] explored the effect of Ta microalloying

Table 4
Summary of Key Research Findings on factors influencing he in welded regions of HSTs.

Factor	Ref.	Research Question	Studied characteristics	Key findings
Material Composition	Liu et al. [154]	How do alloying elements (Cr and Ti) affect HE and microstructure in welded low-alloy steel?	▪ Microstructure analysis ▪ Grain characteristics ▪ Engineering stress–strain ▪ Fracture modes	▪ Ti joints exhibited lower HE sensitivity than Cr joints. ▪ In air, both joints showed ductile fracture surfaces; in hydrogen environments, both shifted to brittle fractures, with larger cracks observed in hydrogen compared to air.
	Beidokhti et al. [155]	How do varying titanium contents and manganese levels affect the HIC and sulfide stress cracking (SSC) susceptibility of submerged arc welded API 5 L-X70 pipeline steel?	▪ Microstructure analysis ▪ HIC & SSC susceptibility ▪ Vickers microhardness	A microstructure rich in acicular ferrite with finely dispersed Ti-carbonitrides and controlled alloying (1.40 % Mn–0.08 % Ti and 1.92 % Mn–0.02 % Ti) maximizes resistance to HIC/SSC in sour environments, while excessive Ti/Mn increased hard phases and raising hardness and susceptibility.
Welding Processes	Christ et al. [156]	How does HE susceptibility vary in gas metal arc welded joints of high-strength low-alloy steel (S690QL) under different welding heat inputs?	▪ Microstructure Analysis ▪ Hardness profiles ▪ Fracture surface	▪ A significant reduction in fracture elongation was observed in all hydrogen-charged specimens relative to the uncharged reference samples. ▪ Higher welding heat input leads to a higher HE susceptibility due to soft WM, severe coarse-grain HAZ hardening, and increased microstructural heterogeneity.
Heat Treatment	Wang et al. [157]	What role does post-weld annealing play in improving HE resistance in the nugget zone of FSW medium-Mn steel?	▪ Microstructure Analysis ▪ Hydrogen permeation characteristics ▪ Fracture morphologies	▪ The as-welded NZ, consisting solely of martensite, was highly susceptible to hydrogen embrittlement, with the highest HE index (HEI) of 79.2 %. ▪ Post-welding annealing introduced reversed austenite, which acted as a strong hydrogen trap, significantly improving HE resistance.
	Guo et al. [158]	How does microstructural variation induced by welding-simulated heat treatments affect the HE sensitivity of S690QL structural steel and X80 pipeline steel under in-situ HC conditions?	▪ Microstructure Analysis ▪ Mechanical Properties ▪ Fracture morphologies	▪ Welding heat treatment increased high angle grain boundaries, reduced ductility. - X80 (slow cooling) showed higher strength and retains HE resistance due to precipitation hardening. - Hydrogen shifts fracture from ductile to cleavage-dominated.
Residual Stresses (RS)	Javadi et al. [159]	How does welding RS influence the size and morphology of HIC for multi-pass TIG welded samples?	▪ RS measurements ▪ Microstructure Analysis	There was a direct correlation between higher RS and larger/more severe hydrogen-induced cracking. The study demonstrated that modifying RS profiles (e.g., through design or processing parameters) can effectively reduce HIC risk in welds.
	Jiang et al. [160]	How does residual tensile stress affect the diffusion and accumulation of hydrogen in thick butt-welded high-strength steel plates?	▪ Residual stress distribution ▪ Hydrogen concentration distribution	▪ The butt weld toe was the weakest area in the thick high-strength steel plate, where high hydrostatic stress and stress concentration encouraged hydrogen cracking. ▪
Weld Defects	Wang et al. [161]	How do common welding defects affect the susceptibility of welded joints, specifically X80 pipeline steel, to HE?	▪ Types of welding defects ▪ Mechanical behavior under slow strain rate tensile (SSRT) ▪ Fracture morphologies ▪ HE Susceptibility Index (IHE)	▪ Defects in welds can greatly increase girth welds' sensitivity to HE and can shift the crack initiation from the specimen surface to the defect sites.

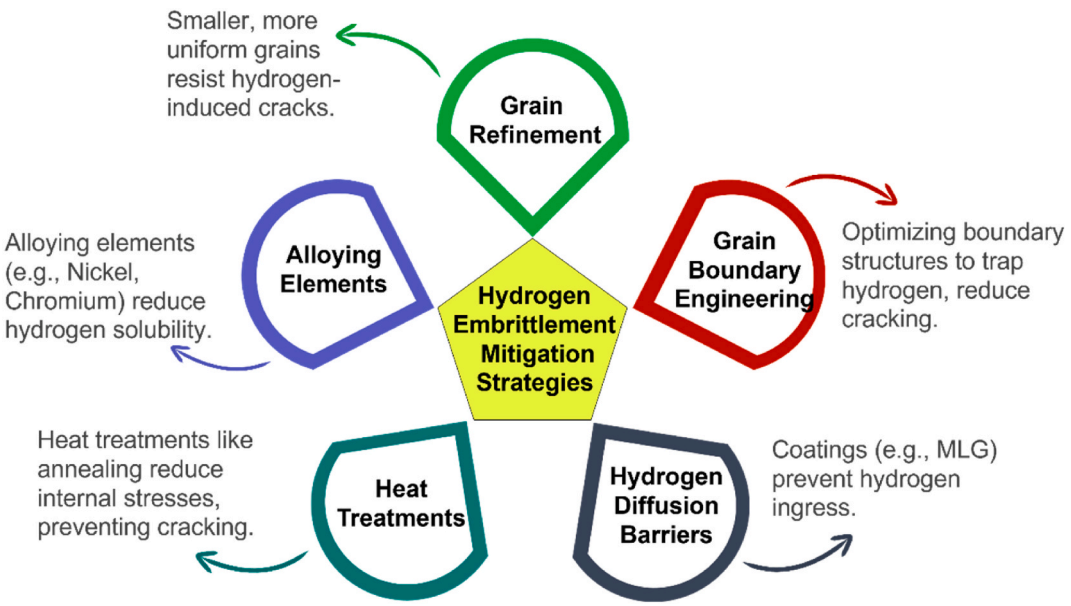

Fig. 6. Mitigation strategies for HE in engineering materials.

on improving HE resistance in lath martensitic steel. Increasing Ta content led to the formation of dispersed nano-sized TaC precipitates and an increase in the martensite/prior austenite grain boundary areas, both of which enhanced hydrogen trapping. The study showed that TaC precipitates provided dominant irreversible hydrogen traps, significantly reducing HEDE compared to reversible traps from microstructural refinement. Additionally, Ta microalloying improved resistance to hydrogen-assisted crack propagation by increasing Σ11 boundaries, low-angle GBs, and reducing Σ3 boundaries, while also hindering hydrogen-dislocation interactions. Wang et al. [171] used first-principles calculations to examine the interactions between 25 different solutes and hydrogen (H) at the Σ5 (310) GB of body-centered cubic (BCC) iron, aiming to understand how solutes influence H behavior and mitigate H-induced GB embrittlement. The study found that elements such as Cr, Mn, Ni, Zr, Nb, Mo, W, and Re reduce H segregation at GBs and enhance resistance to H embrittlement. Conversely, elements like Mg, Sc, As, Pb, and Bi increased H segregation, promoting brittle fracture. The work highlights the importance of specific alloying elements in mitigating H embrittlement and offers guidance for designing materials with improved H resistance. Kim et al. [172] reported that Ni-alloying can overcome the critical challenge of HE by lowering the cathodic reduction rate on the steel surface and slowing hydrogen infusion kinetics in the steel matrix. However, conflicting results arise when steel with a higher Ni content ($\geq$1 wt%) is exposed to neutral-corrosive environments, and these results have not been verified using conventional metallurgical approaches. This study proposes a mechanism for these conflicting results and provides a new, economical strategy for superior resistance to corrosion-induced HE by optimally using Ni-alloying in ultra-strong steel.

6.4. Heat treatments

Heat treatments like annealing and hydrogen stress relief are also vital in mitigating HE. Annealing processes modify the material's microstructure, reducing dislocation density and improving ductility, which makes the material more resistant to cracking when exposed to hydrogen. In addition, hydrogen stress relief (or hydrogen baking) is often employed, where materials are heated in a controlled hydrogen atmosphere to release absorbed hydrogen and reduce internal stresses. This process helps to alleviate the buildup of hydrogen within the material, further enhancing its resistance to embrittlement. Zhou et al. [173] investigated the influence of heat treatment on the HE susceptibility of selective laser melted 18Ni-300 maraging steel. They found that solution treatment led to grain growth and the elimination of the cellular structure, slightly increasing HE susceptibility. In contrast, direct aging and solution-aging processes resulted in the formation of Ni_3(Ti, Mo) precipitates, which enhanced hydrogen trapping. Direct aging, in particular, caused localized austenite aggregation near molten pool boundaries, significantly increasing HE susceptibility. They concluded that heat treatments alter hydrogen trapping sites and diffusion behavior, with direct aging showing the highest HE susceptibility due to hydrogen-assisted cracking. Zhao et al. [174] investigated the effect of tempering on the HE behavior of hot-rolled and intercritically annealed medium-Mn steel (0.1C-5Mn) through slow strain rate tensile testing. The study revealed that tempering reduced the susceptibility to HE, with the most significant elongation loss occurring in the as-annealed specimen. As tempering temperature increased, the hydrogen-induced brittle fracture decreased, and the steel became nearly immune to HE at 500 °C. This improvement was attributed to the microstructural evolution of retained austenite and cementite during tempering. The findings suggest that tempering treatment after intercritical annealing can significantly reduce HE susceptibility without compromising the strength-ductility balance, making it a viable strategy for automotive steel applications. Wang et al. [175] studied the effect of quenching-tempering (QT) treatment on the HE resistance of reactor pressure vessel steel. Transmission electron microscopy and atom probe tomography revealed the decomposition of M3C/VC carbides and the precipitation of M7C3 carbides. Tensile testing showed that HE sensitivity was significantly reduced after the QT treatment. The improved resistance to HE was primarily attributed to the decreased number of M3C carbides, which act as reversible hydrogen traps, as evidenced by the lower concentration of reversible hydrogen measured by TDS. While the amount of irreversible hydrogen also decreased, it was not considered a significant factor in improving HE resistance.

6.5. Hydrogen diffusion barriers

Finally, hydrogen diffusion barriers play a significant role in protecting materials from hydrogen ingress. By applying coatings or surface treatments, engineers can create a protective barrier that significantly reduces the amount of hydrogen that reaches the material. Coatings made from metals such as nickel or chromium can be highly effective in

this regard, preventing hydrogen from diffusing into the base material and thus reducing the risk of embrittlement. These coatings provide an additional layer of protection, especially in environments where hydrogen is present at high concentrations. Shi et al. [176] explored a method for in situ deposition of multi-layered graphene (MLG) coatings on X70 pipe steel to mitigate HE. Carbon was implanted into a nickel catalytic layer on the steel surface, followed by annealing to form MLG. The resulting coatings displayed interpenetrating graphene layers that enhanced adhesion and hydrogen resistance. The MLG coatings significantly reduced hydrogen diffusion and permeability, with diffusion reduced by 123 times and permeability by 48 times. Slow strain rate tests confirmed that the MLG coatings provided strong resistance to HE by inhibiting hydrogen evolution, extending diffusion paths, and improving hydrogen adsorption. Additionally, electrochemical tests showed improved corrosion resistance. These findings highlight MLG coatings as an effective solution to protect commercial steels from HE. Lei et al. [177] conducted a theoretical analysis on the hydrogen permeability of various coatings used in transmission pipelines to mitigate HE. They tested twelve commercially available coatings, including crosslinked poly (vinyl alcohol) (PVA), poly (vinyl chloride) (PVC), and epoxy coatings. Among them, the crosslinked PVA coating demonstrated the lowest hydrogen permeability of 0.0084 Barrer, indicating its highest potential for preventing HE. Mathematical modeling of hydrogen diffusion through coated steel showed that a 2 mm PVA coating could delay hydrogen equilibrium for seven years, reducing hydrogen concentration by 44 % on the steel surface. Further reductions in hydrogen permeability could extend this time even more, providing enhanced protection against HE. This analysis suggests that coatings with low hydrogen permeability, such as crosslinked PVA, are promising candidates for protecting steel pipelines. Behera et al. [178] evaluated the potential of brush-plated ZnNi coatings as a replacement for cadmium (Cd) coatings in preventing internal HE (IHE) of high-strength steel components. They studied the influence of deposition voltage, surface preparation, and anode type on coating microstructure, which plays a crucial role in mitigating IHE. Transmission Electron Microscopy (TEM) and other techniques such as Incremental Step Load (ISL) testing, permeation measurements, and TDS were used to assess hydrogen diffusion and mechanical performance. The study found that coatings deposited at 6 V, with certain surface preparation methods, showed minimal hydrogen generation and did not cause IHE, regardless of microstructure. In contrast, coatings deposited at higher voltages (10 V and 12 V) with certain microstructural features like stacking faults and dislocations were less effective at trapping hydrogen and led to increased IHE risk. The presence of twin boundaries, however, reduced hydrogen diffusion and IHE risk. This research suggests that carefully controlling plating parameters can enable ZnNi coatings to replace Cd coatings without causing IHE in high-strength steel.

7. Modeling of hydrogen diffusion in welds

Hydrogen diffuses through materials due to molecular motion, typically entering interstitial lattice sites or accumulating at microstructural defects such as vacancies, grain boundaries, dislocations, voids, and cracks. In metallic systems, atomic hydrogen can also recombine to form molecular hydrogen within voids or cracks. Defects like dislocations and grain boundaries, which can accommodate a finite amount of hydrogen, are referred to as *saturable traps*. In an ideal, defect-free lattice, hydrogen diffusion occurs via jumps between interstitial sites, requiring sufficient activation energy (E_a) to overcome the energy barrier. Experimental and theoretical studies have shown that under applied stress, hydrogen tends to migrate from regions of lower to higher hydrostatic stress, a process classified as non-steady-state diffusion. This stress-assisted diffusion can be described by a modified form of Fick's second law:

$$\frac{\partial c}{\partial t} = D\nabla^2 c - \frac{DV_m}{RT}(\nabla c \nabla \sigma_h) \tag{9}$$

Here, c represents the concentration, t is time, D denotes the diffusion coefficient, V_m is the partial molar volume of hydrogen in a particular alloy, and σ_h stands for the hydrostatic stress. Under steady-state conditions, its concentration in lattice sites can be estimated using Fick's law. The hydrogen flux vector ($\bar{J}$) is given as:

$$\bar{J} = -D\nabla c \tag{10}$$

The hydrogen diffusion coefficient depends on temperature, position, and time, and is commonly estimated using an Arrhenius-type equation for simplicity

$$D = D_0 e^{\left(-\frac{E_a}{RT}\right)} \tag{11}$$

where D_0 denotes the pre-exponential factor, T is the absolute temperature, E_a is the activation energy to move between two adjacent lattice sites, R is the universal gas constant. The hydrostatic stress gradient (σ_h) arising from material stress facilitates hydrogen diffusion into regions of higher σ_h. Under these conditions, the equation modified accordingly as follows:

$$\bar{J} = -D\nabla c + \frac{DV_m c}{RT}\nabla \sigma_h \tag{12}$$

During diffusion, the total number of HAs remains conserved. In transient diffusion, the hydrogen concentration can vary with time at different locations. Therefore, Equation (1) must be modified to account for changes in hydrogen flux. The gradient of hydrogen flux at the surface is gives as

$$\frac{\partial \bar{J}}{\partial x} dx = J_{out} - J_{in} \tag{13}$$

where J_{out} and J_{in} denote hydrogen flux at the exit and entry surface, respectively. Assuming a constant hydrogen diffusion coefficient, the change in concentration over time can be expressed as follows:

$$\frac{\partial c}{\partial t} = -\nabla . \bar{J} = D\nabla^2 c \tag{14}$$

In the presence of mechanical stresses, the previous equation is modified as follows:

$$\frac{\partial c}{\partial t} = D\nabla^2 c - D\nabla\left(\frac{V_m c}{RT}\nabla \sigma_h\right) \tag{15}$$

This is equivalent to Fick's second law introduced in Equation (1). Thermodynamically, a site is classified as a hydrogen trap if its chemical potential is lower than that of a typical interstitial site. Structural defects such as vacancies, dislocations, and GBs serve as hydrogen traps by increasing the activation energy barrier for diffusion. Grain boundaries, particularly those with high misorientation, are especially significant due to their ability to act as preferential diffusion pathways and their widespread presence in metallic lattices. Vacancies can readily accommodate HAs, with their trapping capacity dependent on the size of the vacancy. This trapping effect results in a decrease in the overall hydrogen diffusion coefficient. Dislocations, which emerge from processes like plastic deformation or grain growth, cause lattice distortions and generate local hydrostatic stress fields. These defects create numerous trapping sites, acting as reversible traps at their edges and irreversible traps at their cores, depending on the local energy conditions. Furthermore, the hydrogen trapping and release behavior is influenced by both the quantity and size of precipitates, with larger precipitates able to retain greater amounts of hydrogen.

McNabb and Foster introduced a hydrogen diffusion model for iron that incorporates trapping sites by treating diffusion as a balance of

sources and sinks, which Oriani later refined by introducing the concept of local equilibrium between mobile and trapped hydrogen [179]. As most hydrogen diffusion models build on these foundations, Fick's laws must be adapted to account for trapping effects. When the hydrogen concentration within trap sites C is assumed to be nonzero, Equation (14) is modified as follows:

$$\frac{\partial(c+C)}{\partial t} = -\nabla.\bar{J} \tag{16}$$

Assuming a constant value for D within the material, Equation (8) can be rewritten as:

$$\frac{\partial c}{\partial t} + \frac{\partial C}{\partial t} = D\nabla^2 c \tag{17}$$

Under the influence of mechanical stresses, the equation is modified as follows:

$$\frac{\partial c}{\partial t} + \frac{\partial C}{\partial t} = D\nabla^2 c + D\nabla\left(\frac{V_m c}{RT}\nabla\sigma_h\right) \tag{18}$$

The fractional occupancy of the traps (ϑ), as proposed by McNabb and Foster, is given by the following equation:

$$\frac{\partial \vartheta}{\partial t} = kc(1-\vartheta) - p\vartheta \tag{19}$$

Here, p and k are parameters that define the trapping effect, with p the probability of trap release within 1 s and k representing the hydrogen capture rate per second and they are given as follows:

$$p = p_0 e^{\left(-\frac{E_d}{RT}\right)} \tag{20}$$

$$k = k_0 e^{\left(-\frac{E_t}{RT}\right)} \tag{21}$$

where E_d is the trapping energy of the site and E_t is the diffusion sites energy. Oriani reformulated the model by assuming that the trap site concentration C depends solely on the lattice hydrogen concentration, with their equilibrium described by a constant K:

$$K = \frac{1-\theta}{\theta}\left(\frac{\vartheta}{1-\vartheta}\right) \tag{22}$$

where θ denotes the occupancy of lattice sites. The hydrogen transport equation can be implemented by drawing an analogy with the heat conduction equation [180]. Due to the mathematical similarity between the two, hydrogen diffusion can be effectively simulated using any finite element method (FEM) software that supports heat transfer analysis. This approach enables the modeling of hydrogen behavior in complex geometries and under various boundary conditions without requiring custom diffusion solvers. The heat equation can be expressed as follows:

$$\rho c_p \frac{\partial T}{\partial t} + \nabla.\overline{J_q} + r_q = 0 \tag{23}$$

In the heat equation, temperature T is replaced by lattice hydrogen concentration c in the diffusion model. By setting density ρ and specific heat c_p to one, the thermal conductivity corresponds to the hydrogen diffusion coefficient D. The heat source term r_q becomes the hydrogen source r_m, typically set to zero, and the heat flux J_q is analogous to the hydrogen flux J. The heat equation, given in Equation (23), is transformed into:

$$\frac{\partial c}{\partial t} + \nabla.\bar{J} + r_m = 0 \tag{24}$$

Based on the aforementioned mathematical modeling, hydrogen diffusion in welded joints is a complex process influenced by a combination of material properties, mechanical stresses, and thermal conditions, all of which interact through well-established physical laws as tabulated in Table 5. The mobile hydrogen concentration in the lattice (c) and the concentration of trapped hydrogen (C) are fundamental variables that govern how hydrogen migrates through the metal. The diffusion coefficient D, which is strongly temperature-dependent via an Arrhenius-type relationship, determines the rate of diffusion and is influenced by the activation energy E_a and pre-exponential factor D_0.

Microstructural defects such as vacancies, dislocations, grain boundaries, and precipitates act as hydrogen traps, reducing the effective diffusion rate by capturing hydrogen atoms. The dynamics of trapping are characterized by parameters such as the trapping rate k, release rate p, and the trapping and desorption energies E_t and E_d, which collectively determine how readily hydrogen is immobilized or released. The trap occupancy ϑ and equilibrium constant K (from Oriani's model) describe the distribution between mobile and trapped hydrogen, depending on the local hydrogen concentration and trap characteristics.

In welded joints, mechanical factors like hydrostatic stress σ_h and its gradient $\nabla\sigma_h$ play a key role, as they drive hydrogen toward regions of higher stress, such as the HAZ. This stress-assisted diffusion must be included in models to accurately predict hydrogen accumulation. Lastly, temperature T not only enhances hydrogen mobility by increasing D, but also modulates trapping behavior via changes in k, p, and K. Taken together, these variables define the intricate hydrogen transport behavior in welded microstructures, and must be fully considered in both analytical and numerical modeling approaches.

Simulation approaches have become an essential tool for studying HE in weldments and materials used in hydrogen tanks. These computational methods enable researchers to predict the behavior of materials

Table 5
Variables influencing hydrogen diffusion in welded joints.

Category	Variable	Symbol	Effect on Diffusion
Material Properties	Hydrogen concentration (lattice)	C	Drives diffusion via concentration gradient; affected by traps and stress.
	Trapped hydrogen concentration	C	Represents hydrogen immobilized in traps; reduces mobile hydrogen.
	Diffusion coefficient	D	Controls how fast hydrogen diffuses; varies with T and trap conditions.
	Activation energy for diffusion	E_a	Higher EaE_a = lower D = slower diffusion.
	Pre-exponential factor	D_0	Material-dependent constant affecting diffusion rate.
	Partial molar volume of hydrogen	V_m	Appears in stress-assisted diffusion term.
	Trap occupancy	ϑ	Fraction of filled traps; influences mobile hydrogen.
	Trap release rate	p	Rate at which hydrogen escapes traps; higher p = more mobile H.
	Trapping rate	k	Rate at which H atoms are trapped; higher k = more trapping.
	Trap energy (desorption)	E_d	Higher EdE_d = deeper traps = more hydrogen immobilized.
	Trap energy (capture)	E_t	Affects how easily hydrogen enters a trap.
	Trap equilibrium constant	K	Relates lattice and trap occupancy under equilibrium.
	Lattice site occupancy	θ	Affects the distribution of hydrogen between mobile and trapped states.
Mechanical	Hydrostatic stress	σ_h	Drives hydrogen into high-stress regions; a key factor in stress-assisted diffusion.
	Stress gradient	$\nabla\sigma_h$	Facilitates directional migration of hydrogen.
Thermal	Temperature	T	Affects D, trap dynamics (k and p), and equilibrium (K); higher T = faster diffusion.

under hydrogen exposure without the need for exhaustive experimental testing. One key simulation approach is finite element analysis (FEA), which is used to model the stress and strain distribution in complex welded structures under hydrogen exposure [181,182]. FEA can help predict areas where hydrogen-induced cracks are likely to initiate, particularly in regions with high residual stresses such as the HAZ. This approach can also incorporate material property variations across different regions of the weldment and account for the effects of temperature gradients and hydrogen pressure. Gobbi et al. [183] presented a fully coupled cohesive zone implementation for the Abaqus FEA code, combining thermal-stress analysis with mass diffusion and heat transfer analogies. The implementation utilizes FORTRAN user subroutines and Python scripts to manage data. A practical example is provided through a FEA model of a fracture toughness test on a compact tension specimen charged with atomic hydrogen, along with a sensitivity analysis to demonstrate the model's ability to predict HE. The model accounts for the interaction between hydrogen diffusion and stress-strain during crack propagation. It uses five user subroutines to compute hydrogen concentration and transfer it to cohesive elements, simulating HE mechanisms. The paper outlines the methodology and showcases the model's predictive capabilities under various conditions. Yu et al. [184] employed FEA simulations to model the temperature field during welding, helping to explain the observed microstructural differences in WMs used in liquid HSTs. The study focuses on three welding methods: Gas Tungsten Arc Welding (GTAW), Submerged Arc Welding (SAW), and Shielded Metal Arc Welding (SMAW). Results show that GTAW and SMAW produce similar microstructures, while SAW leads to larger grains with a more pronounced preferential orientation. Weaving techniques played a significant role in shaping the solidification microstructures. The hardness of the WM is comparable to the base material, with a slight decrease linked to increased grain size. This research offers valuable insights into optimizing welding processes for liquid HSTs, particularly in relation to microstructural characteristics that influence weld joint performance. Alvaro et al. [185] investigated HE susceptibility of a weld-simulated X70 HAZ under high-pressure hydrogen gas at 20 °C. The research combines experimental fracture mechanics testing with modeling and simulation to analyze the effects of hydrogen pressure and exposure time on fracture toughness as shown in Fig. 7 (A). The modeling efforts included 3D FE simulations of hydrogen diffusion, incorporating stress-driven effects. The governing equation (Eq. 25) extended Fick's law to account for hydrostatic stress gradients [187]:

$$\frac{\partial C}{\partial t} = D\nabla^2 C + D\frac{V_H}{R(T-T^2)}\nabla C\nabla p + D\frac{V_H}{R(T-T^2)}C\nabla^2 p \tag{25}$$

Where C is hydrogen concentration, D is diffusion coefficient, V_H is partial molar volume, and p is hydrostatic stress. The simulations revealed that hydrogen concentration near the crack tip reached steady state within 8 h, aligning with experimental failure times. Analytical calculations (Eq. (26)) estimated trapped hydrogen populations using plastic strain-dependent trap densities:

$$\log(N_T) = 23.26 - 2.33 \cdot e^{-5.5 \cdot \varepsilon_p} \tag{26}$$

where N_T is trap site density and ε_p is plastic strain. Trapped hydrogen concentrations were orders of magnitude higher than lattice concentrations, suggesting their dominant role in HE. However, the time-dependent failure implied that lattice hydrogen diffusion also contributed significantly. The study concluded that HE in X70 HAZ is driven by synergistic effects of stress, trapped hydrogen, and lattice diffusion. The simulations provided critical insights into hydrogen distribution and kinetics, supporting the experimental findings. Štěpán Major [186] investigates the fracture modeling of welds affected by hydrogen embrittlement and cyclic loading, presenting three distinct models to simulate the combined effects of hydrogen embrittlement and fatigue as shown in Fig. 7 (B). The study focuses on the degradation processes in welded structures, emphasizing the role of hydrogen diffusion and its impact on material strength. The first model addresses hydrogen-assisted fatigue crack initiation at subsurface inclusions. Hydrogen accumulates in microcavities around inclusions, creating pressure that reduces the stress intensity factor K required for crack growth. The model employs fracture mechanics to describe crack propagation, using a modified Paris-Erdogan equation (Eq. 27) for the initiation phase:

$$N_i(FS, a) = N_{Tot}(FS) - \int_a^{a_f} \frac{da}{C_{PE}(\Delta K)^n} \tag{27}$$

Where C_{PE} and n are material constants, and ΔK is the stress intensity factor. The model incorporates hydrogen transport equations (Eq. 28):

$$\frac{\partial}{\partial t}\int_V (C_L + C_T)\, dV + \int_V \vec{J}\cdot\vec{n}\, dS = 0 \tag{28}$$

where C_L and C_T represent hydrogen concentrations in lattice and trap sites, respectively, and $\vec{J}$ is the hydrogen flux vector. The second model focuses on microvoid coalescence, where hydrogen stabilizes vacancies, forming hydrogen-vacancy complexes that lead to crack initiation. This model uses the crack tip opening displacement (COD) method to calculate the J-integral (Eq. (29)):

$$J_i = \frac{1}{d_N} \cdot \sigma_y \cdot COD_i \tag{29}$$

Where σ_y is the yield strength. The stress tensor is derived using HRR field theory (Eq. (30)):

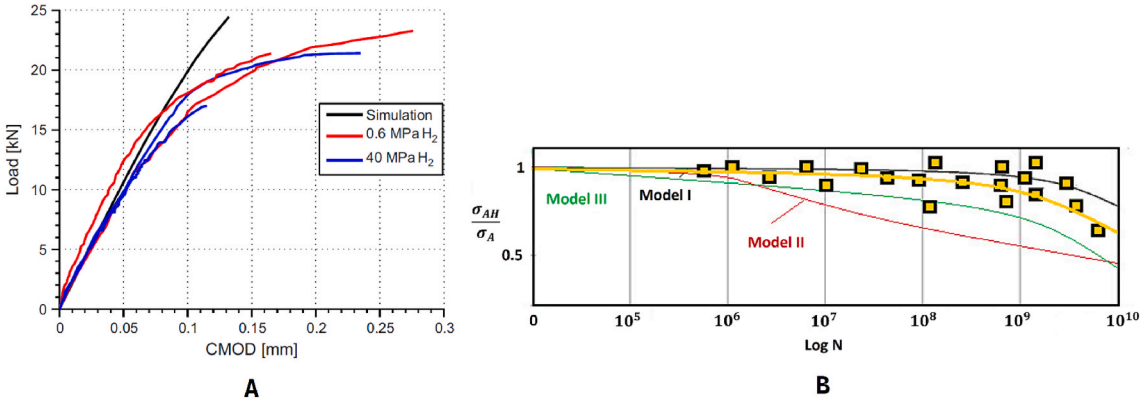

Fig. 7. (A) Comparison of crack mouth opening displacement versus load for SENT tests and simulations [185] (B) Relative decrease in loading amplitude over life: experimental data (yellow) and theoretical predictions for Models 1 (black), 2 (red), and 3 (green) [186].

$$\sigma_{ij} = \left[\frac{E\,.\,J}{\alpha\,.\,\sigma^{*}.\,I_N.\,r}\right]^{\frac{1}{1+N}} . \widetilde{\sigma}_{ij\left(N_{final},\Theta\right)} \tag{30}$$

The third model, based on continuum mechanics, introduces a dimensionless internal variable $\dot{\phi}$ to describe fracture evolution (Eq. (31)):

$$\dot{\phi} = A.\,\gamma^{P} \tag{31}$$

Where A is the accumulation modulus during plastic flow (Eq. (32)), dependent on hydrogen concentration C_L and stress state:

$$A = A\left(C_L, \frac{\sigma_M}{\tau_{eq}}\right) \tag{32}$$

This model predicts fracture perpendicular to the maximum principal tensile stress and is noted for its accuracy in simulating hydrogen embrittlement effects. Experimental validation was performed on welded 16Mo3 steel samples subjected to bending stress and hydrogen exposure. The results showed that Model III (continuum mechanics) provided the most accurate predictions, closely aligning with experimental data, while Model I tended to overestimate allowable loads. Model II, though useful for reconstructing fracture processes, was less effective for lifetime predictions.

8. Conclusion

Hydrogen embrittlement (HE) remains a critical challenge in the safe and reliable deployment of hydrogen storage tanks, particularly in welded joints where metallurgical transformations, residual stresses, and microstructural heterogeneity heighten susceptibility. This review has consolidated current knowledge of HE fundamentals, underlying mechanisms, and their impact on the mechanical integrity of storage materials, showing that welded regions can suffer up to a 20–50 % loss in ductility and significantly higher crack initiation rates compared to base metals. The analysis highlights how hydrogen diffusion, stress concentration zones, and microstructural features interact in complex ways, making welded areas particularly vulnerable. Experimental techniques and simulation models have advanced understanding of HE behavior, but difficulties remain in replicating service conditions and correlating laboratory data with long-term performance. Mitigation strategies; including alloy optimization, improved welding procedures, post-weld heat treatments, and protective coatings; have shown measurable benefits, yet their effectiveness varies with alloy system and environmental exposure. Overall, the findings underscore the multifaceted nature of HE and the need for an integrated, interdisciplinary approach that combines material design, process control, and surface protection to enhance the long-term reliability of hydrogen storage infrastructure.

9. Future research directions and challenges

Future research should prioritize the development of standardized testing protocols that accurately simulate service conditions of hydrogen storage tanks, particularly for welded regions. Advanced characterization techniques at the nanoscale, such as atom probe tomography and in-situ microscopy under hydrogen environments, can provide deeper insights into hydrogen behavior at critical sites like GBs and weld interfaces. Moreover, there is a need for more robust multi-scale modeling frameworks that integrate microstructural features, mechanical loading, and hydrogen diffusion to predict HE more accurately. Investigating the long-term performance of mitigation strategies under cyclic loading and variable pressure-temperature conditions is also essential for real-world validation. Additionally, exploring the role of novel materials, including high-entropy alloys and hydrogen-resistant composites, could open new pathways toward embrittlement-resistant tank designs. Collaborations between materials scientists, mechanical engineers, and industry stakeholders will be crucial in translating research findings into practical design guidelines and safety standards for next-generation hydrogen storage systems.

CRediT authorship contribution statement

Ammar Elsheikh: Conceptualization, Investigation, Methodology, Visualization, Writing – original draft, Writing – review & editing. **Ali Ali:** Formal analysis, Funding acquisition, Resources, Writing – original draft. **Fadl A. Essa:** Investigation, Methodology, Writing – original draft. **Mohamed A.E. Omer:** Investigation, Methodology, Writing – original draft. **Mohamed G. Abou-Ali:** Methodology, Writing – original draft. **Ninshu Ma:** Conceptualization, Investigation, Writing – review & editing.

Declaration of competing interest

The authors of the submitted manuscript declared that there is no conflict of interest.

Acknowledgement

This work was partially supported by “Osaka University promotion program of cutting-edge multilateral international collaboration related to joining and materials science” and “JWRI International Joint Research Collaborators (JIJReC) program.".

Data availability

No data was used for the research described in the article.

References

[1] M. Al-Emran, C. Griffy-Brown, The role of technology adoption in sustainable development: overview, opportunities, challenges, and future research agendas, Technol. Soc. 73 (2023) 102240, https://doi.org/10.1016/j.techsoc.2023.102240.
[2] W. Jiang, S. Chen, P. Tang, Y. Hu, M. Liu, S. Qiu, M. Iqbal, Role of natural resources, renewable energy sources, eco-innovation and carbon taxes in carbon neutrality: evidence from G7 economies, Heliyon 10 (2024) e33526, https://doi.org/10.1016/j.heliyon.2024.e33526.
[3] X.H. Chen, K. Tee, M. Elnahass, R. Ahmed, Assessing the environmental impacts of renewable energy sources: a case study on air pollution and carbon emissions in China, J. Environ. Manag. 345 (2023) 118525, https://doi.org/10.1016/j.jenvman.2023.118525.
[4] E. Kim, H. Jamal, I. Jeon, F. Khan, S.E. Chun, J.H. Kim, Functionality of 1-Butyl-2,3-Dimethylimidazolium bromide (BMI-Br) as a solid plasticizer in PEO-based polymer electrolyte for highly reliable lithium metal batteries, Adv. Energy Mater. 13 (2023) 2301674, https://doi.org/10.1002/AENM.202301674.
[5] S. Kim, H. Jamal, F. Khan, A. Al-Ahmed, M.M. Abdelnaby, A. Al-Zahrani, S. E. Chun, J.H. Kim, Achieving high durability in all-solid-state lithium metal batteries using metal–organic framework solid polymer electrolytes, J Mater Chem A Mater 12 (2024) 10942–10955, https://doi.org/10.1039/D3TA07184G.
[6] A. Afif, S.M. Rahman, A. Tasfiah Azad, J. Zaini, M.A. Islam, A.K. Azad, Advanced materials and technologies for hybrid supercapacitors for energy storage – a review, J. Energy Storage 25 (2019) 100852, https://doi.org/10.1016/J.EST.2019.100852.
[7] W. Smith, The role of fuel cells in energy storage, J. Power Sources 86 (2000) 74–83, https://doi.org/10.1016/S0378-7753(99)00485-1.
[8] J. Mei, T. Liao, H. Peng, Z. Sun, Bioinspired materials for energy storage, Small Methods 6 (2022) 2101076, https://doi.org/10.1002/SMTD.202101076.
[9] H. Wei, D. Cui, J. Ma, L. Chu, X. Zhao, H. Song, H. Liu, T. Liu, N. Wang, Z. Guo, Energy conversion technologies towards self-powered electrochemical energy storage systems: the state of the art and perspectives, J Mater Chem A Mater 5 (2017) 1873–1894, https://doi.org/10.1039/C6TA09726J.
[10] O.A. Ibrahim, M. Navarro-Segarra, P. Sadeghi, N. Sabaté, J.P. Esquivel, E. Kjeang, Microfluidics for electrochemical energy conversion, Chem Rev 122 (2022) 7236–7266, https://doi.org/10.1021/ACS.CHEMREV.1C00499.
[11] K.M. Kennedy, M.A. Borrero, M.R. Edwards, P. O'Rourke, N.E. Hultman, K. Surana, Advancing equitable value chains for the global hydrogen economy, Energy and Climate Change 5 (2024) 100166, https://doi.org/10.1016/j.egycc.2024.100166.
[12] E. Abbasian Hamedani, S.A. Alenabi, S. Talebi, Hydrogen as an energy source: a review of production technologies and challenges of fuel cell vehicles, Energy Rep. 12 (2024) 3778–3794, https://doi.org/10.1016/j.egyr.2024.09.030.

[13] M. Yue, H. Lambert, E. Pahon, R. Roche, S. Jemei, D. Hissel, Hydrogen energy systems: a critical review of technologies, applications, trends and challenges, Renew. Sustain. Energy Rev. 146 (2021) 111180, https://doi.org/10.1016/j.rser.2021.111180.
[14] M.A. Habib, G.A.Q. Abdulrahman, A.B.S. Alquaity, N.A.A. Qasem, Hydrogen combustion, production, and applications: a review, Alex. Eng. J. 100 (2024) 182–207, https://doi.org/10.1016/j.aej.2024.05.030.
[15] B. Reda, A.A. Elzamar, S. AlFazzani, S.M. Ezzat, Green hydrogen as a source of renewable energy: a step towards sustainability, an overview, Environ. Dev. Sustain. (2024), https://doi.org/10.1007/s10668-024-04892-z.
[16] M. El-Shafie, Hydrogen production by water electrolysis technologies: a review, Results Eng. 20 (2023) 101426, https://doi.org/10.1016/j.rineng.2023.101426.
[17] L. Mulky, S. Srivastava, T. Lakshmi, E.R. Sandadi, S. Gour, N.A. Thomas, S. Shanmuga Priya, K. Sudhakar, An overview of hydrogen storage technologies – key challenges and opportunities, Mater. Chem. Phys. 325 (2024) 129710, https://doi.org/10.1016/j.matchemphys.2024.129710.
[18] K.T. Møller, T.R. Jensen, E. Akiba, H. Li, Hydrogen - a sustainable energy carrier, Prog. Nat. Sci. Mater. Int. 27 (2017) 34–40, https://doi.org/10.1016/j.pnsc.2016.12.014.
[19] A. Magliano, C. Perez Carrera, C.M. Pappalardo, D. Guida, V.P. Berardi, A comprehensive literature review on hydrogen tanks: storage, safety, and structural integrity, Appl. Sci. 14 (2024), https://doi.org/10.3390/app14209348.
[20] T. Zhang, J. Uratani, Y. Huang, L. Xu, S. Griffiths, Y. Ding, Hydrogen liquefaction and storage: recent progress and perspectives, Renew. Sustain. Energy Rev. 176 (2023) 113204, https://doi.org/10.1016/j.rser.2023.113204.
[21] E. harrak Abdechafik, H. Ait Ousaleh, S. Mehmood, Y. Filali Baba, I. Bürger, M. Linder, A. Faik, An analytical review of recent advancements on solid-state hydrogen storage, Int. J. Hydrogen Energy 52 (2024) 1182–1193, https://doi.org/10.1016/j.ijhydene.2023.10.218.
[22] H. Sun, Z. Wang, Q. Meng, S. White, Advancements in hydrogen storage technologies: enhancing efficiency, safety, and economic viability for sustainable energy transition, Int. J. Hydrogen Energy 105 (2025) 10–22, https://doi.org/10.1016/j.ijhydene.2025.01.176.
[23] A.I. Osman, M. Nasr, A.S. Eltaweil, M. Hosny, M. Farghali, A.S. Al-Fatesh, D. W. Rooney, E.M. Abd El-Monaem, Advances in hydrogen storage materials: harnessing innovative technology, from machine learning to computational chemistry, for energy storage solutions, Int. J. Hydrogen Energy 67 (2024) 1270–1294, https://doi.org/10.1016/j.ijhydene.2024.03.223.
[24] Y.-S. Chen, C. Huang, P.-Y. Liu, H.-W. Yen, R. Niu, P. Burr, K.L. Moore, E. Martínez-Pañeda, A. Atrens, J.M. Cairney, Hydrogen trapping and embrittlement in metals – a review, Int. J. Hydrogen Energy (2024), https://doi.org/10.1016/j.ijhydene.2024.04.076.
[25] A. Campari, F. Ustolin, A. Alvaro, N. Paltrinieri, A review on hydrogen embrittlement and risk-based inspection of hydrogen technologies, Int. J. Hydrogen Energy 48 (2023) 35316–35346, https://doi.org/10.1016/j.ijhydene.2023.05.293.
[26] P.C. Okonkwo, E.M. Barhoumi, I. Ben Belgacem, I.B. Mansir, M. Aliyu, W. Emori, P.C. Uzoma, W.H. Beitelmal, E. Akyüz, A.B. Radwan, R.A. Shakoor, A focused review of the hydrogen storage tank embrittlement mechanism process, Int. J. Hydrogen Energy 48 (2023) 12935–12948, https://doi.org/10.1016/j.ijhydene.2022.12.252.
[27] U.S. Meda, N. Bhat, A. Pandey, K.N. Subramanya, M.A. Lourdu Antony Raj, Challenges associated with hydrogen storage systems due to the hydrogen embrittlement of high strength steels, Int. J. Hydrogen Energy 48 (2023) 17894–17913, https://doi.org/10.1016/j.ijhydene.2023.01.292.
[28] P.C. Okonkwo, E.M. Barhoumi, I. Ben Belgacem, I.B. Mansir, M. Aliyu, W. Emori, P.C. Uzoma, W.H. Beitelmal, E. Akyüz, A.B. Radwan, R.A. Shakoor, A focused review of the hydrogen storage tank embrittlement mechanism process, Int. J. Hydrogen Energy 48 (2023) 12935–12948, https://doi.org/10.1016/J.IJHYDENE.2022.12.252.
[29] Y. Sun, Y. Frank Cheng, Hydrogen-induced degradation of high-strength steel pipeline welds: a critical review, Eng. Fail. Anal. 133 (2022) 105985, https://doi.org/10.1016/J.ENGFAILANAL.2021.105985.
[30] G. Jia, M. Lei, M. Li, W. Xu, R. Li, Y. Lu, M. Cai, Hydrogen embrittlement in hydrogen-blended natural gas transportation systems: a review, Int. J. Hydrogen Energy 48 (2023) 32137–32157, https://doi.org/10.1016/J.IJHYDENE.2023.04.266.
[31] H. Yu, A. Díaz, X. Lu, B. Sun, Y. Ding, M. Koyama, J. He, X. Zhou, A. Oudriss, X. Feaugas, Z. Zhang, Hydrogen embrittlement as a conspicuous material challenge—comprehensive review and future directions, Chem Rev 124 (2024) 6271–6392, https://doi.org/10.1021/ACS.CHEMREV.3C00624.
[32] Q. Cheng, R. Zhang, Z. Shi, J. Lin, Review of common hydrogen storage tanks and current manufacturing methods for aluminium alloy tank liners, Int. J. Lightweight Mater. Manuf. 7 (2024) 269–284, https://doi.org/10.1016/J.IJLMM.2023.08.002.
[33] T. Amirthan, M.S.A. Perera, The role of storage systems in hydrogen economy: a review, J. Nat. Gas Sci. Eng. 108 (2022) 104843, https://doi.org/10.1016/J.JNGSE.2022.104843.
[34] T. Amirthan, M.S.A. Perera, The role of storage systems in hydrogen economy: a review, J. Nat. Gas Sci. Eng. 108 (2022) 104843, https://doi.org/10.1016/j.jngse.2022.104843.
[35] X. Li, X. Ma, J. Zhang, E. Akiyama, Y. Wang, X. Song, Review of hydrogen embrittlement in metals: hydrogen diffusion, hydrogen characterization, hydrogen embrittlement mechanism and prevention, Acta Metall. Sin. 33 (2020) 759–773, https://doi.org/10.1007/s40195-020-01039-7.
[36] S.K. Dwivedi, M. Vishwakarma, Hydrogen embrittlement in different materials: a review, Int. J. Hydrogen Energy 43 (2018) 21603–21616, https://doi.org/10.1016/j.ijhydene.2018.09.201.
[37] V. Balaji, P. Jeyapandiarajan, J. Joel, A. Anbalagan, P. Ashwath, S. Margret Anouncia, A. Batako, M. Anthony Xavior, Mitigating hydrogen embrittlement in high-entropy alloys for next-generation hydrogen storage systems, J. Mater. Res. Technol. 33 (2024) 7681–7697, https://doi.org/10.1016/j.jmrt.2024.11.139.
[38] H.J. Wan, X.Q. Wu, H.L. Ming, J.Q. Wang, E.H. Han, Effects of hydrogen charging time and pressure on the hydrogen embrittlement susceptibility of X52 pipeline steel material, Acta Metall. Sin. 37 (2024) 293–307, https://doi.org/10.1007/S40195-023-01625-5/METRICS.
[39] S.K. Dwivedi, M. Vishwakarma, Hydrogen embrittlement in different materials: a review, Int. J. Hydrogen Energy 43 (2018) 21603–21616, https://doi.org/10.1016/J.IJHYDENE.2018.09.201.
[40] H. Yu, A. Díaz, X. Lu, B. Sun, Y. Ding, M. Koyama, J. He, X. Zhou, A. Oudriss, X. Feaugas, Z. Zhang, Hydrogen embrittlement as a conspicuous material challenge—comprehensive review and future directions, Chem Rev 124 (2024) 6271–6392, https://doi.org/10.1021/ACS.CHEMREV.3C00624/ASSET/IMAGES/MEDIUM/CR3C00624_0044.GIF.
[41] R.K.Z. Davani, E. Entezari, M.A. Mohtadi-Bonab, S. Yadav, J.F.A. Cabezas, J. Szpunar, Effect of electrochemical hydrogen charging on hydrogen embrittlement and mechanical properties of quenched tempered X100 pipeline steel, J. Fail. Anal. Prev. 24 (2024) 318–330, https://doi.org/10.1007/S11668-023-01841-2/METRICS.
[42] G. Yi, Y. Xu, C. Zheng, H. Ma, D. Ju, J. Zhang, X. Hu, Study on the influence of electrochemical charging conditions on the hydrogen embrittlement behavior of X65MS pipeline steel, J. Mater. Eng. Perform. (2025) 1–13, https://doi.org/10.1007/S11665-025-11509-7/METRICS.
[43] S.Y. Lee, B. Hwang, Hydrogen embrittlement of three high-manganese steels tested by different hydrogen charging methods, J. Kor. Inst. Met. Mater. 55 (2017) 695–702, https://doi.org/10.3365/KJMM.2017.55.10.695.
[44] Y. Zhao, J.M. Park, D.H. Lee, E.J. Song, J.Y. Suh, U. Ramamurty, J. il Jang, Influences of hydrogen charging method on the hydrogen distribution and nanomechanical properties of face-centered cubic high-entropy alloy: a comparative study, Scr. Mater. 168 (2019) 76–80, https://doi.org/10.1016/J.SCRIPTAMAT.2019.04.025.
[45] S. Rahimi, K. Verbeken, T. Depover, E. Proverbio, Hydrogen embrittlement of pipeline steels under gaseous and electrochemical charging: a comparative review on tensile properties, Eng. Fail. Anal. 167 (2025) 108956, https://doi.org/10.1016/J.ENGFAILANAL.2024.108956.
[46] Z. Feng, X. Li, X. Song, T. Gu, Y. Zhang, Hydrogen embrittlement of CoCrFeMnNi high-entropy alloy compared with 304 and IN718 alloys, Metals 12 (2022) 998, https://doi.org/10.3390/MET12060998, 998 12 (2022).
[47] H. Ma, H. Tian, Z. Wang, K. He, Y. Wang, Q. Zhang, D. Liu, Z. Cui, Effect of electrochemical hydrogen charging on blistering and mechanical properties behavior of Q690 steel, Crystals 13 (2023), https://doi.org/10.3390/cryst13060918.
[48] V. Olden, C. Thaulow, R. Johnsen, Modelling of hydrogen diffusion and hydrogen induced cracking in supermartensitic and duplex stainless steels, Mater. Des. 29 (2008) 1934–1948, https://doi.org/10.1016/J.MATDES.2008.04.026.
[49] C.F. Dong, Z.Y. Liu, X.G. Li, Y.F. Cheng, Effects of hydrogen-charging on the susceptibility of X100 pipeline steel to hydrogen-induced cracking, Int. J. Hydrogen Energy 34 (2009) 9879–9884, https://doi.org/10.1016/J.IJHYDENE.2009.09.090.
[50] R. Walallawita, M.C. Hinchliff, D. Sediako, J. Quinn, V. Chou, K. Walker, Hydrogen embrittlement in vintage grade 290 pipeline steel and its welded region via ex-situ and in-situ testing, Eng. Fail. Anal. 173 (2025) 109410, https://doi.org/10.1016/J.ENGFAILANAL.2025.109410.
[51] R. Walallawita, M.C. Hinchliff, D. Sediako, J. Quinn, V. Chou, K. Walker, Hydrogen embrittlement in vintage grade 290 pipeline steel and its welded region via ex-situ and in-situ testing, Eng. Fail. Anal. 173 (2025) 109410, https://doi.org/10.1016/J.ENGFAILANAL.2025.109410.
[52] A. Zafra, G. Álvarez, G. Benoit, G. Henaff, E. Martinez-Pañeda, C. Rodríguez, J. Belzunce, Hydrogen-assisted fatigue crack growth: pre-Charging vs in-situ testing in gaseous environments, Mater. Sci. Eng., A 871 (2023) 144885, https://doi.org/10.1016/J.MSEA.2023.144885.
[53] D.H. Lee, J.Y. Jung, K.H. Lee, S.Y. Lee, Y. Zhao, K.B. Lau, P. Wang, U. Ramamurty, Distinct effects of in-situ and ex-situ hydrogen charging methods on the mechanical behavior of CoCrFeNi high-entropy alloy fabricated by laser-powder bed fusion, J. Alloys Compd. 940 (2023) 168858, https://doi.org/10.1016/J.JALLCOM.2023.168858.
[54] M. Christ, X. Guo, R. Sharma, T. Li, W. Bleck, U. Reisgen, Hydrogen embrittlement susceptibility of gas metal arc welded joints from a high-strength low-alloy steel grade S690QL, Steel Res. Int. 91 (2020) 2000131, https://doi.org/10.1002/srin.202000131.
[55] J. Gou, X. Xing, G. Cui, Z. Li, J. Liu, X. Deng, Hydrogen-induced cracking in CGHAZ of welded X80 steel under tension load, Metals 13 (2023), https://doi.org/10.3390/met13071325.
[56] A. Behvar, M. Haghshenas, M.B. Djukic, Hydrogen embrittlement and hydrogen-induced crack initiation in additively manufactured metals: a critical review on mechanical and cyclic loading, Int. J. Hydrogen Energy 58 (2024) 1214–1239, https://doi.org/10.1016/j.ijhydene.2024.01.232.
[57] J. Song, W.A. Curtin, Mechanisms of hydrogen-enhanced localized plasticity: an atomistic study using α-Fe as a model system, Acta Mater. 68 (2014) 61–69, https://doi.org/10.1016/j.actamat.2014.01.008.

[58] M.L. Martin, P. Sofronis, Hydrogen-induced cracking and blistering in steels: a review, J. Nat. Gas Sci. Eng. 101 (2022) 104547, https://doi.org/10.1016/j.jngse.2022.104547.
[59] G. Ghosh, P. Rostron, R. Garg, A. Panday, Hydrogen induced cracking of pipeline and pressure vessel steels: a review, Eng. Fract. Mech. 199 (2018) 609–618, https://doi.org/10.1016/j.engfracmech.2018.06.018.
[60] X. Li, W. Huang, X. Wu, J. Zhang, Y. Wang, E. Akiyama, D. Hou, Effect of hydrogen charging time on hydrogen blister and hydrogen-induced cracking of pure iron, Corros. Sci. 181 (2021) 109200, https://doi.org/10.1016/J.CORSCI.2020.109200.
[61] M.L. Martin, P. Sofronis, Hydrogen-induced cracking and blistering in steels: a review, J. Nat. Gas Sci. Eng. 101 (2022) 104547, https://doi.org/10.1016/J.JNGSE.2022.104547.
[62] M. Elboujdaini, R.W. Revie, Metallurgical factors in stress corrosion cracking (SCC) and hydrogen-induced cracking (HIC), J. Solid State Electrochem. 13 (2009) 1091–1099, https://doi.org/10.1007/S10008-009-0799-0/FIGURES/14.
[63] F. Huang, J. Liu, Z.J. Deng, J.H. Cheng, Z.H. Lu, X.G. Li, Effect of microstructure and inclusions on hydrogen induced cracking susceptibility and hydrogen trapping efficiency of X120 pipeline steel, Mater. Sci. Eng., A 527 (2010) 6997–7001, https://doi.org/10.1016/J.MSEA.2010.07.022.
[64] F. Fagnoni, E.C. Kursun, M. Busi, P. Konarski, O. Yetik, R. Spolenak, J. Bertsch, L. I. Duarte, Hydrogen enhanced localized plasticity in zirconium as observed by digital image correlation, J. Nucl. Mater. 590 (2024) 154873, https://doi.org/10.1016/J.JNUCMAT.2023.154873.
[65] M.L. Martin, M. Dadfarnia, A. Nagao, S. Wang, P. Sofronis, Enumeration of the hydrogen-enhanced localized plasticity mechanism for hydrogen embrittlement in structural materials, Acta Mater. 165 (2019) 734–750, https://doi.org/10.1016/J.ACTAMAT.2018.12.014.
[66] S. Huang, Y. Zhang, C. Yang, H. Hu, Fracture strain model for hydrogen embrittlement based on hydrogen enhanced localized plasticity mechanism, Int. J. Hydrogen Energy 45 (2020) 25541–25554, https://doi.org/10.1016/J.IJHYDENE.2020.06.271.
[67] L. Deconinck, X. Lu, D. Wang, R. Johnsen, K. Verbeken, T. Depover, Hydrogen enhanced localised plasticity of single grain α titanium verified by in-situ hydrogen microcantilever bending, Int. J. Hydrogen Energy 136 (2025) 902–913, https://doi.org/10.1016/J.IJHYDENE.2024.03.135.
[68] M. Solnørdal, S. Wästberg, G. Heiberg, O. Hauås-Eide, Hydrogen induced stress cracking (HISC) and DNV-RP-F112, Measurement and Control 42 (2009) 145–148, https://doi.org/10.1177/002029400904200504.
[69] R. Johnsen, Hydrogen induced stress cracking of stainless steel in seawater-what do we know and what is still unknown, in: The Annual Congress of the European Federation of Corrosion, 20th International Corrosion Congress and Process Safety Congress, 2017.
[70] X. Dong, D. Wang, P. Thoudden-Sukumar, A. Tehranchi, D. Ponge, B. Sun, D. Raabe, Hydrogen-associated decohesion and localized plasticity in a high-Mn and high-Al two-phase lightweight steel, Acta Mater. 239 (2022) 118296, https://doi.org/10.1016/J.ACTAMAT.2022.118296.
[71] H. Khalid, B. Mansoor, Hydrogen embrittlement in nickel-base superalloy 718, Recent Developments in Analytical Techniques for Corrosion Research (2022) 279–306, https://doi.org/10.1007/978-3-030-89101-5_13/FIGURES/20.
[72] K.S. Chan, J. Moody, A hydrogen-induced decohesion model for treating cold dwell fatigue in titanium-based alloys, Metall Mater Trans A Phys Metall Mater Sci 47 (2016) 2058–2072, https://doi.org/10.1007/S11661-016-3367-0/FIGURES/20.
[73] Q. Tan, S. He, X. Chen, Y. Liu, O.I. Gorbatov, P. Peng, Hydrogen-enhanced decohesion mechanism of the Ni-Ni3X interfaces in precipitation-hardened Ni-based alloys, J. Alloys Compd. 963 (2023) 171186, https://doi.org/10.1016/J.JALLCOM.2023.171186.
[74] A.S. Kholtobina, W. Ecker, R. Pippan, V.I. Razumovskiy, Effect of alloying elements on hydrogen enhanced decohesion in bcc iron, Comput. Mater. Sci. 188 (2021) 110215, https://doi.org/10.1016/J.COMMATSCI.2020.110215.
[75] X. Li, W. Huang, X. Wu, J. Zhang, Y. Wang, E. Akiyama, D. Hou, Effect of hydrogen charging time on hydrogen blister and hydrogen-induced cracking of pure iron, Corros. Sci. 181 (2021) 109200, https://doi.org/10.1016/j.corsci.2020.109200.
[76] X.C. Ren, Q.J. Zhou, G.B. Shan, W.Y. Chu, J.X. Li, Y.J. Su, L.J. Qiao, A nucleation mechanism of hydrogen blister in metals and alloys, Metall Mater Trans A Phys Metall Mater Sci 39 (2008) 87–97, https://doi.org/10.1007/S11661-007-9391-3/FIGURES/10.
[77] M.L. Martin, P. Sofronis, Hydrogen-induced cracking and blistering in steels: a review, J. Nat. Gas Sci. Eng. 101 (2022) 104547, https://doi.org/10.1016/J.JNGSE.2022.104547.
[78] X. Li, X. Ma, J. Zhang, E. Akiyama, Y. Wang, X. Song, Review of hydrogen embrittlement in metals: hydrogen diffusion, hydrogen characterization, hydrogen embrittlement mechanism and prevention, Acta Metall. Sin. 33 (2020) 759–773, https://doi.org/10.1007/S40195-020-01039-7/METRICS.
[79] I.S. Batra, R.N. Singh, P. Sengupta, B.C. Maji, K. Madangopal, K.V. Manikrishna, R. Tewari, G.K. Dey, Mitigation of hydride embrittlement of zirconium by yttrium, J. Nucl. Mater. 389 (2009) 500–503, https://doi.org/10.1016/J.JNUCMAT.2009.02.036.
[80] S. Nazar, E. Proverbio, Modeling of hydrogen-assisted fatigue crack growth in carbon steel pipelines, Int. J. Hydrogen Energy 138 (2025) 548–558, https://doi.org/10.1016/J.IJHYDENE.2025.05.205.
[81] L.W. Tsay, J.J. Chen, J.C. Huang, Hydrogen-assisted fatigue crack growth of AISI 316L stainless steel weld, Corros. Sci. 50 (2008) 2973–2980, https://doi.org/10.1016/J.CORSCI.2008.08.016.
[82] Z. Fu, P. Wu, Q. Yang, Q. Kan, G. Kang, Hydrogen-assisted fatigue crack propagation behavior of selective laser–melted inconel 718 alloy, Corros. Sci. 227 (2024) 111745, https://doi.org/10.1016/J.CORSCI.2023.111745.
[83] R. Fernández-Sousa, C. Betegón, E. Martínez-Pañeda, Analysis of the influence of microstructural traps on hydrogen assisted fatigue, Acta Mater. 199 (2020) 253–263, https://doi.org/10.1016/J.ACTAMAT.2020.08.030.
[84] S.S. Shishvan, G. Csányi, V.S. Deshpande, Hydrogen induced fast-fracture, J. Mech. Phys. Solid. 134 (2020) 103740, https://doi.org/10.1016/J.JMPS.2019.103740.
[85] R.G. Song, M.K. Tseng, B.J. Zhang, J. Liu, Z.H. Jin, K.S. Shin, Grain boundary segregation and hydrogen-induced fracture in 7050 aluminium alloy, Acta Mater. 44 (1996) 3241–3248, https://doi.org/10.1016/1359-6454(95)00406-8.
[86] M.R. Bache, W.J. Evans, H.M. Davies, Electron back scattered diffraction (EBSD) analysis of quasi-cleavage and hydrogen induced fractures under cyclic and dwell loading in titanium alloys, J. Mater. Sci. 32 (1997) 3435–3442, https://doi.org/10.1023/A:1018624801310/METRICS.
[87] J. Venezuela, T. Hill, Q. Zhou, H. Li, Z. Shi, F. Dong, R. Knibbe, M. Zhang, M. S. Dargusch, A. Atrens, Hydrogen-induced fast fracture in notched 1500 and 1700 MPa class automotive martensitic advanced high-strength steel, Corros. Sci. 188 (2021) 109550, https://doi.org/10.1016/J.CORSCI.2021.109550.
[88] X.Y. Zhou, J.H. Zhu, H.H. Wu, X.S. Yang, S. Wang, X. Mao, Unveiling the role of hydrogen on the creep behaviors of nanograined α-Fe via molecular dynamics simulations, Int. J. Hydrogen Energy 46 (2021) 9613–9629, https://doi.org/10.1016/J.IJHYDENE.2020.12.115.
[89] M.M. Hall, HYDROGEN ASSISTED CREEP FRACTURE MODEL FOR LOW POTENTIAL STRESS CORROSION CRACKING OF ni-cr-fe ALLOYS. https://www.researchgate.net/publication/260293182, 2001. (Accessed 19 June 2025).
[90] N. Pushilina, A. Panin, M. Syrtanov, E. Kashkarov, V. Kudiiarov, O. Perevalova, R. Laptev, A. Lider, A. Koptyug, Hydrogen-induced phase transformation and microstructure evolution for Ti-6Al-4V parts produced by electron beam melting, Metals 8 (2018), https://doi.org/10.3390/met8050301.
[91] E. Hong, D.C. Dunand, H. Choe, Hydrogen-induced transformation superplasticity in zirconium, Int. J. Hydrogen Energy 35 (2010) 5708–5713, https://doi.org/10.1016/J.IJHYDENE.2010.03.088.
[92] W. Li, X. Zhu, C. Wang, X. Jin, Effect of S-phase on the hydrogen induced phase transition and hydrogen embrittlement susceptibility in AISI 304 stainless steel, Mater. Today Proc. 2 (2015) S691–S695, https://doi.org/10.1016/J.MATPR.2015.07.377.
[93] N. Pushilina, A. Panin, M. Syrtanov, E. Kashkarov, V. Kudiiarov, O. Perevalova, R. Laptev, A. Lider, A. Koptyug, Hydrogen-induced phase transformation and microstructure evolution for Ti-6Al-4V parts produced by Electron beam melting, Metals 8 (2018) 301, https://doi.org/10.3390/MET8050301, 301 8 (2018).
[94] A.R. Mazza, Q. Lu, G. Hu, H. Li, J.F. Browning, T.R. Charlton, M. Brahlek, P. Ganesh, T.Z. Ward, H.N. Lee, G. Eres, Reversible hydrogen-induced phase transformations in La0.7Sr0.3MnO3Thin films characterized by in Situ Neutron reflectometry, ACS Appl. Mater. Interfaces 14 (2022) 10898–10906, https://doi.org/10.1021/ACSAMI.1C20590/ASSET/IMAGES/LARGE/AM1C20590_0006.JPEG.
[95] Z. Jiang, H. Li, F. Yu, K. Ma, X. Shu, S. Li, Z. Yang, B. Xiao, Effect of creep stress level on hydrogen embrittlement mechanism of Al-Zn-Mg-Cu alloy, Mater. Sci. Eng., A 920 (2025) 147542, https://doi.org/10.1016/J.MSEA.2024.147542.
[96] N.-E. Laadel, M. El Mansori, N. Kang, S. Marlin, Y. Boussant-Roux, Permeation barriers for hydrogen embrittlement prevention in metals – a review on mechanisms, materials suitability and efficiency, Int. J. Hydrogen Energy 47 (2022) 32707–32731, https://doi.org/10.1016/j.ijhydene.2022.07.164.
[97] Z.A. Luo, L.Y. Mao, C. Huang, H.Y. Zhou, M.K. Wang, A strategy for simultaneously enhancing mechanical strength and hydrogen embrittlement resistance: exceptional performance of laminated metal composite in hydrogen environments, Mater. Des. 237 (2024) 112549, https://doi.org/10.1016/j.matdes.2023.112549.
[98] Y. Zhu, G. Liu, Z. Cui, H. Yang, F. Liu, B. Jiang, L. Chen, Effect and mechanism of ionic liquid-polymer composite coating on enhancing hydrogen embrittlement resistance of X80 pipeline steel for hydrogen blended natural gas transportation, Int. J. Hydrogen Energy 80 (2024) 1305–1316, https://doi.org/10.1016/j.ijhydene.2024.07.091.
[99] M. Elkhodbia, G. Mubarak, I. Gadala, I. Barsoum, A. AlFantazi, A. Al Tamimi, Experimental and computational failure analysis of hydrogen embrittled steel cords in a reinforced thermoplastic composite pipe, Eng. Fail. Anal. 157 (2024) 107962, https://doi.org/10.1016/j.engfailanal.2024.107962.
[100] N. Kapuscinsky, P. Ignatusha, A. Islam, M. Ezzine, N. Du, K.M. Meek, Polymeric coatings for preventing hydrogen embrittlement in industrial storage and transmission systems, ACS Applied Engineering Materials 2 (2024) 2488–2503.
[101] Z. Cao, Z. Wang, Y. Ngiam, Z. Luo, Z. Geng, J. Wang, Y. Zhang, M. Huang, Hydrogen embrittlement evaluation and prediction in press-hardened steels, Steel Res. Int. 94 (2023) 2200685, https://doi.org/10.1002/srin.202200685.
[102] M.B. Djukic, V. Sijacki Zeravcic, G.M. Bakic, A. Sedmak, B. Rajicic, Hydrogen damage of steels: a case study and hydrogen embrittlement model, Eng. Fail. Anal. 58 (2015) 485–498, https://doi.org/10.1016/j.engfailanal.2015.05.017.
[103] M. Koyama, E. Akiyama, Y.-K. Lee, D. Raabe, K. Tsuzaki, Overview of hydrogen embrittlement in high-Mn steels, Int. J. Hydrogen Energy 42 (2017) 12706–12723, https://doi.org/10.1016/j.ijhydene.2017.02.214.
[104] G.A. Young, J.R. Scully, The effects of test temperature, temper, and alloyed copper on the hydrogen-controlled crack growth rate of an Al-Zn-Mg-(Cu) alloy, Metall. Mater. Trans. 33 (2002) 1167–1181, https://doi.org/10.1007/s11661-002-0218-y.

[105] J. Yamabe, D. Takagoshi, H. Matsunaga, S. Matsuoka, T. Ishikawa, T. Ichigi, High-strength copper-based alloy with excellent resistance to hydrogen embrittlement, Int. J. Hydrogen Energy 41 (2016) 15089–15094, https://doi.org/10.1016/j.ijhydene.2016.05.156.
[106] X. Lu, Y. Ma, D. Wang, On the hydrogen embrittlement behavior of nickel-based alloys: alloys 718 and 725, Mater. Sci. Eng., A 792 (2020) 139785, https://doi.org/10.1016/j.msea.2020.139785.
[107] H.L. Mai, X.-Y. Cui, D. Scheiber, L. Romaner, S.P. Ringer, An understanding of hydrogen embrittlement in nickel grain boundaries from first principles, Mater. Des. 212 (2021) 110283, https://doi.org/10.1016/j.matdes.2021.110283.
[108] E. Tal-Gutelmacher, D. Eliezer, The hydrogen embrittlement of titanium-based alloys, JOM 57 (2005) 46–49, https://doi.org/10.1007/s11837-005-0115-0.
[109] X. Liu, J. Wang, L. Gao, R. Li, X. Luo, W. Zhang, X. Zhang, X. Zha, Surface concentration and microscale distribution of hydrogen and the associated embrittlement in a near α titanium alloy, J. Alloys Compd. 862 (2021) 158669, https://doi.org/10.1016/j.jallcom.2021.158669.
[110] J. Kim, D. Hall, H. Yan, Y. Shi, S. Joseph, S. Fearn, R.J. Chater, D. Dye, C.C. Tasan, Roughening improves hydrogen embrittlement resistance of Ti-6Al-4V, Acta Mater. 220 (2021) 117304, https://doi.org/10.1016/j.actamat.2021.117304.
[111] Q. Cheng, R. Zhang, Z. Shi, J. Lin, Review of common hydrogen storage tanks and current manufacturing methods for aluminium alloy tank liners, Int. J. Lightweight Mater. Manuf. 7 (2024) 269–284, https://doi.org/10.1016/j.ijlmm.2023.08.002.
[112] L. Shi, J. Shuai, X. Wang, K. Xu, Experimental and numerical investigation of stress in a large-scale steel tank with a floating roof, Thin-Walled Struct. 117 (2017) 25–34, https://doi.org/10.1016/j.tws.2017.03.037.
[113] E. Ohaeri, U. Eduok, J. Szpunar, Hydrogen related degradation in pipeline steel: a review, Int. J. Hydrogen Energy 43 (2018) 14584–14617, https://doi.org/10.1016/j.ijhydene.2018.06.064.
[114] M. Okayasu, H. Matsuura, Hydrogen embrittlement properties of several stainless steels, Int. J. Fract. 248 (2024) 201–220, https://doi.org/10.1007/s10704-024-00809-z.
[115] R. Urbanczyk, K. Peinecke, M. Felderhoff, K. Hauschild, W. Kersten, S. Peil, D. Bathen, Aluminium alloy based hydrogen storage tank operated with sodium aluminium hexahydride Na3AlH6, Int. J. Hydrogen Energy 39 (2014) 17118–17128, https://doi.org/10.1016/j.ijhydene.2014.08.101.
[116] J. Liu, M. Zhao, L. Rong, Overview of hydrogen-resistant alloys for high-pressure hydrogen environment: on the hydrogen energy structural materials, Clean Energy 7 (2023) 99–115, https://doi.org/10.1093/ce/zkad009.
[117] L. Liu, L.N. Li, X. Liu, X.D. Shu, C. Xie, Atomistic modeling of hydrogen embrittlement at grain boundaries of Mg, J. Mater. Res. Technol. 33 (2024) 9762–9773, https://doi.org/10.1016/j.jmrt.2024.11.240.
[118] H. Momida, Y. Asari, Y. Nakamura, Y. Tateyama, T. Ohno, Hydrogen-enhanced vacancy embrittlement of grain boundaries in iron, Phys. Rev. B 88 (2013) 144107, https://doi.org/10.1103/PhysRevB.88.144107.
[119] S. Bechtle, M. Kumar, B.P. Somerday, M.E. Launey, R.O. Ritchie, Grain-boundary engineering markedly reduces susceptibility to intergranular hydrogen embrittlement in metallic materials, Acta Mater. 57 (2009) 4148–4157, https://doi.org/10.1016/j.actamat.2009.05.012.
[120] I. Taji, T. Hajilou, S. Karimi, F. Schott, E. Plesiutschnig, A. Barnoush, R. Johnsen, Role of grain boundaries in hydrogen embrittlement of alloy 725: single and bi-crystal microcantilever bending study, Int. J. Hydrogen Energy 47 (2022) 12771–12781, https://doi.org/10.1016/j.ijhydene.2022.01.251.
[121] X. Xi, Z. Liu, Z. Qin, T. Wu, J. Wang, N. Xu, L. Chen, Enhancement of the resistance to hydrogen embrittlement by tailoring grain boundary characteristics in a low carbon high strength steel, J. Mater. Res. Technol. 27 (2023) 7119–7127, https://doi.org/10.1016/j.jmrt.2023.11.156.
[122] S. Manda, S. Kumar, R.R. Tripathy, B. Sudhalkar, N.N. Pai, S. Basu, A. Durgaprasad, D. Vijayshankar, A.S. Panwar, I. Samajdar, Origin of hydrogen embrittlement in ferrite-martensite dual-phase steel, Int. J. Hydrogen Energy 100 (2025) 1266–1281, https://doi.org/10.1016/j.ijhydene.2024.12.411.
[123] L.X. Li, Y.H. Wang, W.J. Wang, J.Y. Liu, Z.Q. Xu, F.S. Du, Mechanism and prediction of hydrogen embrittlement based on complex phase structure of chromium alloy steel, Mater. Sci. Eng., A 822 (2021) 141546, https://doi.org/10.1016/j.msea.2021.141546.
[124] C. Örnek, M. Mansoor, A. Larsson, F. Zhang, G.S. Harlow, R. Kroll, F. Carlà, H. Hussain, B. Derin, U. Kivisäkk, D.L. Engelberg, E. Lundgren, J. Pan, The causation of hydrogen embrittlement of duplex stainless steel: phase instability of the austenite phase and ductile-to-brittle transition of the ferrite phase – synergy between experiments and modelling, Corros. Sci. 217 (2023) 111140, https://doi.org/10.1016/j.corsci.2023.111140.
[125] Y. Wang, B. Sharma, Y. Xu, K. Shimizu, H. Fujihara, K. Hirayama, A. Takeuchi, M. Uesugi, G. Cheng, H. Toda, Switching nanoprecipitates to resist hydrogen embrittlement in high-strength aluminum alloys, Nat. Commun. 13 (2022) 6860, https://doi.org/10.1038/s41467-022-34628-4.
[126] F. Dong, J. Venezuela, H. Li, Z. Shi, Q. Zhou, L. Chen, J. Chen, L. Du, A. Atrens, The influence of phosphorus on the temper embrittlement and hydrogen embrittlement of some dual-phase steels, Mater. Sci. Eng., A 854 (2022) 143379, https://doi.org/10.1016/j.msea.2022.143379.
[127] F. Ye, T. Zhu, K. Mori, Q. Xu, Y. Song, Q. Wang, R. Yu, B. Wang, X. Cao, Effects of dislocations and hydrogen concentration on hydrogen embrittlement of austenitic 316 stainless steels, J. Alloys Compd. 876 (2021) 160134, https://doi.org/10.1016/j.jallcom.2021.160134.
[128] L. Vandewalle, M.J. Konstantinović, T. Depover, K. Verbeken, The potential of the internal friction technique to evaluate the role of vacancies and dislocations in the hydrogen embrittlement of steels, Steel Res. Int. 92 (2021) 2100037, https://doi.org/10.1002/srin.202100037.
[129] Y. Sugiyama, K. Takai, Quantities and distribution of strain-induced vacancies and dislocations enhanced by hydrogen in iron, Acta Mater. 208 (2021) 116663, https://doi.org/10.1016/j.actamat.2021.116663.
[130] L. Chiari, A. Komatsu, M. Fujinami, Defects responsible for hydrogen embrittlement in austenitic stainless steel 304 by positron annihilation lifetime spectroscopy, ISIJ Int. 61 (2021) 1927–1934.
[131] L. Deconinck, M.T. Villa Vidaller, E. Bernardo Quejido, E.A. Jägle, T. Depover, K. Verbeken, In-situ hydrogen embrittlement evaluation of as-built and heat treated laser powder bed fused Ti-6Al-4V versus conventionally cold rolled Ti-6Al-4V, Addit. Manuf. 76 (2023) 103768, https://doi.org/10.1016/j.addma.2023.103768.
[132] T.-D. Nguyen, C. Singh, D.-H. Lee, Y.S. Kim, T. Lee, S.Y. Lee, Deciphering hydrogen embrittlement mechanisms in Ti6Al4V alloy: role of solute hydrogen and hydride phase, Materials 17 (2024), https://doi.org/10.3390/ma17051178.
[133] L. Deconinck, E. Bernardo Quejido, M.T. Villa Vidaller, E.A. Jägle, K. Verbeken, T. Depover, The mechanism behind the effect of building orientation and surface roughness on hydrogen embrittlement of laser powder bed fused Ti-6Al-4V, Addit. Manuf. 72 (2023) 103613, https://doi.org/10.1016/j.addma.2023.103613.
[134] H. Zhang, C. Leygraf, L. Wen, F. Huang, H. Chang, Y. Jin, The formation of hydride and its influence on Ti–6Al–4V alloy fracture behavior, Int. J. Hydrogen Energy 48 (2023) 36169–36184, https://doi.org/10.1016/j.ijhydene.2023.05.226.
[135] X. Li, J. Zhang, Y. Cui, M.B. Djukic, H. Feng, Y. Wang, Review of the hydrogen embrittlement and interactions between hydrogen and microstructural interfaces in metallic alloys: grain boundary, twin boundary, and nano-precipitate, Int. J. Hydrogen Energy 72 (2024) 74–109, https://doi.org/10.1016/j.ijhydene.2024.05.257.
[136] S. Pichler, A. Bendo, G. Mori, M. Safyari, M. Moshtaghi, Inhibition of grain growth by pearlite improves hydrogen embrittlement susceptibility of the ultra-low carbon ferritic steel: the influence of H-assisted crack initiation and propagation mechanisms, J. Mater. Sci. 58 (2023) 13460–13475, https://doi.org/10.1007/s10853-023-08856-y.
[137] K.-S. Kim, J.-H. Kang, S.-J. Kim, Carbon effect on hydrogen diffusivity and embrittlement in austenitic stainless steels, Corros. Sci. 180 (2021) 109226, https://doi.org/10.1016/j.corsci.2020.109226.
[138] P.-Y. Liu, B. Zhang, R. Niu, S.-L. Lu, C. Huang, M. Wang, F. Tian, Y. Mao, T. Li, P. A. Burr, H. Lu, A. Guo, H.-W. Yen, J.M. Cairney, H. Chen, Y.-S. Chen, Engineering metal-carbide hydrogen traps in steels, Nat. Commun. 15 (2024) 724, https://doi.org/10.1038/s41467-024-45017-4.
[139] M. Pinson, H. Springer, T. Depover, K. Verbeken, The role of cementite on the hydrogen embrittlement mechanism in martensitic medium-carbon steels, Mater. Sci. Eng., A 859 (2022) 144204, https://doi.org/10.1016/j.msea.2022.144204.
[140] E. Rodoni, K. Verbeken, T. Depover, M. Iannuzzi, Effect of microstructure on the hydrogen embrittlement, diffusion, and uptake of dual-phase low alloy steels with varying ferrite-martensite ratios, Int. J. Hydrogen Energy 50 (2024) 53–65, https://doi.org/10.1016/j.ijhydene.2023.07.061.
[141] H.-S. Noh, J.-H. Kang, K.-M. Kim, S.-J. Kim, The effect of carbon on hydrogen embrittlement in stable Cr-Ni-Mn-N austenitic stainless steels, Corros. Sci. 124 (2017) 63–70, https://doi.org/10.1016/j.corsci.2017.05.004.
[142] D.M. Symons, Hydrogen embrittlement of Ni-Cr-Fe alloys, Metall. Mater. Trans. 28 (1997) 655–663, https://doi.org/10.1007/s11661-997-0051-4.
[143] S. Simonetti, C. Lanz, G. Brizuela, Hydrogen embrittlement of a Fe–Cr–Ni alloy: analysis of the physical and chemical processes in the early stage of stress corrosion cracking initiation, Solid State Sci. 15 (2013) 137–141, https://doi.org/10.1016/j.solidstatesciences.2012.10.006.
[144] E. Rodoni, L. Claeys, T. Depover, M. Iannuzzi, Effect of nickel on the hydrogen diffusion, trapping and embrittlement properties of tempered ferritic-martensitic dual-phase low alloy steels, Int. J. Hydrogen Energy 98 (2025) 418–428, https://doi.org/10.1016/j.ijhydene.2024.12.112.
[145] O.I. Balytskyi, L.M. Ivaskevych, Effect of alloying and heat treatment on embrittlement of fe-cr-ni alloys in high-pressure hydrogen, Strength Mater. 55 (2023) 79–89, https://doi.org/10.1007/s11223-023-00504-9.
[146] L.C. Liu, Z.P. Wu, Z.Y. Xu, S.F. Zhou, Effects of W and Mo concentration on hydrogen embrittlement and elastic properties of V membrane, Int. J. Hydrogen Energy 89 (2024) 1105–1111, https://doi.org/10.1016/j.ijhydene.2024.09.413.
[147] L.B. Peral, I. Fernández-Pariente, C. Colombo, C. Rodríguez, J. Belzunce, The positive role of nanometric molybdenum–vanadium carbides in mitigating hydrogen embrittlement in structural steels, Materials 14 (2021), https://doi.org/10.3390/ma14237269.
[148] J. Lee, T. Lee, D.-J. Mun, C.M. Bae, C.S. Lee, Comparative study on the effects of Cr, V, and Mo carbides for hydrogen-embrittlement resistance of tempered martensitic steel, Sci. Rep. 9 (2019) 5219, https://doi.org/10.1038/s41598-019-41436-2.
[149] C.L. Briant, Z.F. Wang, N. Chollocoop, Hydrogen embrittlement of commercial purity titanium, Corros. Sci. 44 (2002) 1875–1888, https://doi.org/10.1016/S0010-938X(01)00159-7.
[150] D.S. Shih, I.M. Robertson, H.K. Birnbaum, Hydrogen embrittlement of α titanium: in situ tem studies, Acta Metall. 36 (1988) 111–124, https://doi.org/10.1016/0001-6160(88)90032-6.
[151] S. Wu, Y. Chen, Y. Yu, J. Tang, Y. Wang, R. Guo, M. Sun, C. Zhao, X. Luo, N. Li, Hydrogen atom occupancy variation induced fragile to strong transition of titanium hydride, Scr. Mater. 243 (2024) 115993, https://doi.org/10.1016/j.scriptamat.2024.115993.

[152] Y. Chen, S. Zhao, H. Ma, H. Wang, L. Hua, S. Fu, Analysis of hydrogen embrittlement on aluminum alloys for vehicle-mounted hydrogen storage tanks: a review, Metals 11 (2021), https://doi.org/10.3390/met11081303.
[153] H. Zhao, P. Chakraborty, D. Ponge, T. Hickel, B. Sun, C.-H. Wu, B. Gault, D. Raabe, Hydrogen trapping and embrittlement in high-strength Al alloys, Nature 602 (2022) 437–441, https://doi.org/10.1038/s41586-021-04343-z.
[154] Z. Liu, Y. Wang, Y. Zhai, N. Pan, Y. Zhang, X. Wang, G. Xu, Role of Ti and Cr on microstructure and hydrogen embrittlement of welded joint of low-alloy steel used for armor layer, Mater. Sci. Eng., A 896 (2024) 146305, https://doi.org/10.1016/j.msea.2024.146305.
[155] B. Beidokhti, A. Dolati, A.H. Koukabi, Effects of alloying elements and microstructure on the susceptibility of the welded HSLA steel to hydrogen-induced cracking and sulfide stress cracking, Mater. Sci. Eng., A 507 (2009) 167–173, https://doi.org/10.1016/J.MSEA.2008.11.064.
[156] M. Christ, X. Guo, R. Sharma, T. Li, W. Bleck, U. Reisgen, Hydrogen embrittlement susceptibility of gas metal arc welded joints from a high-strength low-alloy steel grade S690QL, Steel Res. Int. 91 (2020) 2000131, https://doi.org/10.1002/SRIN.202000131.
[157] Y.Q. Wang, J.X. Su, Z.Q. Jin, R.H. Duan, G.M. Xie, Improved resistance to hydrogen embrittlement in the nugget zone of friction stir welded medium Mn steel via post-welding annealing, Corros. Sci. 227 (2024) 111786, https://doi.org/10.1016/j.corsci.2023.111786.
[158] X. Guo, T. Li, Z. Sheng, M. Christ, R. Sharma, M. Söker, U. Reisgen, W. Bleck, Impact of welding simulated heat treatment on hydrogen embrittlement behavior of high-strength fine-grained steels, Eng. Fail. Anal. 140 (2022) 106602, https://doi.org/10.1016/j.engfailanal.2022.106602.
[159] Y. Javadi, N.E. Sweeney, E. Mohseni, C.N. MacLeod, D. Lines, M. Vasilev, Z. Qiu, C. Mineo, S.G. Pierce, A. Gachagan, Investigating the effect of residual stress on hydrogen cracking in multi-pass robotic welding through process compatible non-destructive testing, J. Manuf. Process. 63 (2021) 80–87, https://doi.org/10.1016/J.JMAPRO.2020.03.043.
[160] J. Jiang, W. Zeng, L. Li, Effect of residual stress on hydrogen diffusion in thick butt-welded high-strength steel plates, Metals 12 (2022) 1074, https://doi.org/10.3390/MET12071074, 1074 12 (2022).
[161] B. Wang, Q. Liu, Q. Feng, X. Wang, Z. Yang, L. Dai, X. Huo, D. Wang, J. Yu, J. Chen, Influence of welding defects on hydrogen embrittlement sensitivity of girth welds in X80 pipelines, Int. J. Electrochem. Sci. 19 (2024) 100661, https://doi.org/10.1016/J.IJOES.2024.100661.
[162] O. Barrera, D. Bombac, Y. Chen, T.D. Daff, E. Galindo-Nava, P. Gong, D. Haley, R. Horton, I. Katzarov, J.R. Kermode, C. Liverani, M. Stopher, F. Sweeney, Understanding and mitigating hydrogen embrittlement of steels: a review of experimental, modelling and design progress from atomistic to continuum, J. Mater. Sci. 53 (2018) 6251–6290, https://doi.org/10.1007/s10853-017-1978-5.
[163] B. Sun, X. Dong, J. Wen, X.-C. Zhang, S.-T. Tu, Microstructure design strategies to mitigate hydrogen embrittlement in metallic materials, Fatig. Fract. Eng. Mater. Struct. 46 (2023) 3060–3076, https://doi.org/10.1111/ffe.14074.
[164] Y.H. Fan, B. Zhang, J.Q. Wang, E.-H. Han, W. Ke, Effect of grain refinement on the hydrogen embrittlement of 304 austenitic stainless steel, J. Mater. Sci. Technol. 35 (2019) 2213–2219, https://doi.org/10.1016/j.jmst.2019.03.043.
[165] Y. Mine, N. Horita, Z. Horita, K. Takashima, Effect of ultrafine grain refinement on hydrogen embrittlement of metastable austenitic stainless steel, Int. J. Hydrogen Energy 42 (2017) 15415–15425, https://doi.org/10.1016/j.ijhydene.2017.04.249.
[166] H. Khalid, V.C. Shunmugasamy, R.W. DeMott, K. Hattar, B. Mansoor, Effect of grain size and precipitates on hydrogen embrittlement susceptibility of nickel alloy 718, Int. J. Hydrogen Energy 55 (2024) 474–490, https://doi.org/10.1016/j.ijhydene.2023.11.233.
[167] Y.J. Kwon, S.-P. Jung, B.-J. Lee, C.S. Lee, Grain boundary engineering approach to improve hydrogen embrittlement resistance in FeMnC TWIP steel, Int. J. Hydrogen Energy 43 (2018) 10129–10140, https://doi.org/10.1016/j.ijhydene.2018.04.048.
[168] Y.J. Kwon, H.J. Seo, J.N. Kim, C.S. Lee, Effect of grain boundary engineering on hydrogen embrittlement in Fe-Mn-C TWIP steel at various strain rates, Corros. Sci. 142 (2018) 213–221, https://doi.org/10.1016/j.corsci.2018.07.028.
[169] Q. Sun, J. Han, J. Li, F. Cao, S. Wang, Tailoring hydrogen embrittlement resistance of pure Ni by grain boundary engineering, Corros. Commun. 6 (2022) 48–51, https://doi.org/10.1016/j.corcom.2022.02.003.
[170] S. Zhang, D. Xu, F. Huang, W. Gao, J. Wan, J. Liu, Mitigation of hydrogen embrittlement in ultra-high strength lath martensitic steel via Ta microalloying, Mater. Des. 210 (2021) 110090, https://doi.org/10.1016/j.matdes.2021.110090.
[171] F. Wang, X. Zhang, C. Zhang, X. Zhou, H.-H. Wu, L. Dong, Y. Zhu, S. Wang, J. Gao, H. Zhao, Y. Huang, H. Lu, A. Guo, X. Mao, Effect of alloy element on hydrogen-induced grain boundary embrittlement in BCC iron, J. Mater. Res. Technol. 33 (2024) 9439–9447, https://doi.org/10.1016/j.jmrt.2024.11.264.
[172] S.J. Kim, E.H. Hwang, J.S. Park, S.M. Ryu, D.W. Yun, H.G. Seong, Inhibiting hydrogen embrittlement in ultra-strong steels for automotive applications by Ni-alloying, npj Mater. Degrad. 3 (2019) 12, https://doi.org/10.1038/s41529-019-0074-5.
[173] N. Zhou, S. Zhang, C. Ma, H. Zhang, C. Wu, J. Liu, F. Huang, Effect of heat treatment on the hydrogen embrittlement susceptibility of selective laser melted 18Ni-300 maraging steel, Mater. Sci. Eng., A 885 (2023) 145622, https://doi.org/10.1016/j.msea.2023.145622.
[174] X. Zhao, Y. Zhang, W. Hui, C. Shao, C. Wang, H. Dong, The potential significance of tempering treatment in alleviating the hydrogen embrittlement susceptibility of a hot-rolled and intercritically annealed medium-Mn steel, Eng. Fail. Anal. 119 (2021) 104969, https://doi.org/10.1016/j.engfailanal.2020.104969.
[175] Y. Wang, S. Hu, Y. Li, G. Cheng, Improved hydrogen embrittlement resistance after quenching–tempering treatment for a Cr-Mo-V high strength steel, Int. J. Hydrogen Energy 44 (2019) 29017–29026, https://doi.org/10.1016/j.ijhydene.2019.09.142.
[176] K. Shi, S. Xiao, Q. Ruan, H. Wu, G. Chen, C. Zhou, S. Jiang, K. Xi, M. He, P.K. Chu, Hydrogen permeation behavior and mechanism of multi-layered graphene coatings and mitigation of hydrogen embrittlement of pipe steel, Appl. Surf. Sci. 573 (2022) 151529, https://doi.org/10.1016/j.apsusc.2021.151529.
[177] Y. Lei, E. Hosseini, L. Liu, C.A. Scholes, S.E. Kentish, Internal polymeric coating materials for preventing pipeline hydrogen embrittlement and a theoretical model of hydrogen diffusion through coated steel, Int. J. Hydrogen Energy 47 (2022) 31409–31419, https://doi.org/10.1016/j.ijhydene.2022.07.034.
[178] P. Behera, S.K. Rajagopalan, S. Brahimi, C.A. Venturella, S.P. Gaydos, R.J. Straw, S. Yue, Effect of brush plating process variables on the microstructures of Cd and ZnNi coatings and hydrogen embrittlement, Surf. Coat. Technol. 417 (2021) 127181, https://doi.org/10.1016/j.surfcoat.2021.127181.
[179] X.Y. Cheng, H.X. Zhang, A new perspective on hydrogen diffusion and hydrogen embrittlement in low-alloy high strength steel, Corros. Sci. 174 (2020) 108800, https://doi.org/10.1016/j.corsci.2020.108800.
[180] P. Cavaliere, A. Perrone, D. Marsano, A. Marzanese, B. Sadeghi, Modelling of the hydrogen embrittlement in austenitic stainless steels, Materialia 30 (2023) 101855, https://doi.org/10.1016/j.mtla.2023.101855.
[181] T. Mente, T. Bollinghaus, Modeling of hydrogen distributionin a duplex stainless steel, Weld. World 56 (2012) 66–78, https://doi.org/10.1007/BF03321397/METRICS.
[182] O. Gen, M. Koki, M. Masahito, M. Yoshiki, I. Kazuhiro, Numerical simulation on effect of microstructure on hydrogen-induced cracking behavior in duplex stainless steel weld metal, ISIJ Int. 61 (2021) 1236–1244, https://doi.org/10.2355/ISIJINTERNATIONAL.ISIJINT-2020-400.
[183] G. Gobbi, C. Colombo, S. Miccoli, L. Vergani, A fully coupled implementation of hydrogen embrittlement in FE analysis, Adv. Eng. Software 135 (2019) 102673, https://doi.org/10.1016/j.advengsoft.2019.04.004.
[184] C. Yu, T. Kawabata, S. Kyouno, X. Li, S. Uranaka, D. Maeda, Influence of welding methods on the microstructure of nickel-based weld metal for liquid hydrogen tanks, J. Mater. Sci. 59 (2024) 22310–22326, https://doi.org/10.1007/s10853-024-10505-x.
[185] A. Alvaro, V. Olden, A. Macadre, Hydrogen embrittlement susceptibility of a weld simulated X70 heat affected zone under H2 pressure, Mater. Sci. Eng., A 597 (2014) 29–36, https://doi.org/10.1016/J.MSEA.2013.12.042.
[186] Š. Major, Fracture modeling of a weld damaged by hydrogen embrittlement, Procedia Struct. Integr. 48 (2023) 230–237, https://doi.org/10.1016/J.PROSTR.2023.07.153.
[187] V. Olden, A. Saai, L. Jemblie, R. Johnsen, FE simulation of hydrogen diffusion in duplex stainless steel, Int. J. Hydrogen Energy 39 (2014) 1156–1163, https://doi.org/10.1016/J.IJHYDENE.2013.10.101.